DEPARTMENT OF THE INTERIOR

UNITED STATES GEOLOGICAL SURVEY

The Laramie Mountains, Wyoming, earthquake of 18 October 1984
A report on its aftershocks and seismotectonic setting

By

C.J. Langer[1], R.A. Martin[2], C.K. Wood[2], G.L. Snyder[3], and G.A. Bollinger[4]

Open-File Report 91-258

[1]U.S.Geological Survey, MS 966, Denver Federal Center, Denver, CO 80225
[2]U.S. Bureau of Reclamation, MC D-1632, Denver Federal Center, Denver, CO 80225
[3]U.S. Geological Survey, MS 913, Denver Federal Center, Denver, CO 80225
[4]U.S. Geological Survey, Denver, CO and Seismological Observatory, Virginia Polytechnic Institute and State University, Blacksburg, VA 24061

1991

CONTENTS

ILLUSTRATIONS

TABLES

The Laramie Mountains, Wyoming, earthquake of 18 October 1984; A report on its aftershocks and seismotectonic setting

by
C.J. Langer, R.A. Martin, C.K. Wood, G.L. Snyder, and G.A. Bollinger

ABSTRACT

A moderate-sized earthquake (m_b = 5.4, M_0 = 1.1 X 10^{24} dyne cm) occurred on 18 October 1984 in the Precambrian complex of granitic rocks in the northern Laramie Mountains of southeastern Wyoming. The earthquake was felt over a broad area (287,000 km^2) but caused only minor damage (MMI_0 = VI at Douglas, Medicine Bow, and vicinity). The unusually deep focus for this shock (~ 22 km) contributes to its somewhat low meizoseismal intensity. A temporary network of sixteen analog and seven digital portable seismographs was installed for more than six days in the epicentral region to record aftershock data. Most hypocenters of the 47 located aftershocks cluster in a cylindrical pattern about 4 km in diameter at depths between 20 and 25 km.

Single-event focal mechanism solutions define two principle classes of aftershock focal mechanisms. Nineteen mechanisms indicate predominantly strike-slip faulting, twelve of which are similar to the main shock focal mechanism (range of azimuth of *T*-axes ~ N. 13° E. - N. 57° E.; range of plunge ~0° - 25°) while twenty-eight mechanisms indicate predominantly normal faulting (range of azimuth of *T*-axes ~ N. 02° E. - N. 68° E.; range of plunge ~1° - 18°). The spatial distribution of aftershocks and strikes of aftershock focal mechanism nodal planes exhibit no obvious correlations with local geologic or topographic features. A geologic field investigation following the main shock sought surficial evidence of Holocene movement on likely ancestral faults possibly related to the earthquake source. Three of the most apparent topographic lineaments near the epicenter were inspected for evidence of fault offsets but no displacements younger than Tertiary were found.

INTRODUCTION

The m_b 5.4 (M_L 5.5) Laramie Mountains earthquake of 18 October 1984 was one of the most severe Wyoming events to occur outside Yellowstone Park in recent time. The historical record shows that it is ranked second only to the 1897 MMI_0 VI-VII earthquake near Casper (see Table 1), some 85 km northwest of the Laramie Mountains epicenter (fig. 1). With exception of the M_s 7.5 Hebgan Lake earthquake in neighboring Montana on 17 August 1959, and some of its aftershocks, Wyoming has been effected by few damaging shocks (five with MMI_0 = VI in the ninety years between 1894 and 1984; listed in Table 1). Most earthquakes within the state occur inside the Intermountain Seismic Belt (e.g. see Smith, 1978), a northerly trending corridor of seismicity west of 110 deg. W. longitude that includes the Yellowstone region (fig. 1a).

The drouth of significant 20th-century seismicity throughout Wyoming ended in 1984 when a series of four moderate-sized earthquakes occurred. No damage resulted from the first two (m_b 5.0, 29 May 1984; m_b 5.1, 8 September 1984), which had epicenters in the Powder River Basin, about 35 km west of Gillette and some 160 km north-northwest from Casper. Slight damage (some broken dishes and glassware) was reported following a fourth event (m_b 5.0, 3 November 1984) centered in the southern Wind River Mountains about 35 km south-southwest of Lander and 200 km west-southwest from Casper. Intensity data gathered by a postcard survey of the two Powder River Basin earthquakes indicated felt areas of 50,000-70,000 km^2 (Stover, 1985); data obtained from the shock near Lander were insufficient to compute an isoseismal distribution. The Laramie Mountains shock was the third event and also largest by 0.3 - 0.4 of a magnitude unit. It was felt over a broad area more than four times the size affected by any of the other three. Its numerous aftershocks included six equal to or greater than magnitude m_b = 3.0.

As reported previously by Langer and others (1985), the aftershock foci were unusually deep (below 20.5 km) for intraplate seismicity in the Western United States. Because of the anomalously large felt area for a magnitude 5.4 earthquake (probably due at least in part to the greater than average focal depth) in the intermountain region, its location near strategic national defense positions around Cheyenne and the presence of dams situated in the regional drainage system, special attention was devoted to an

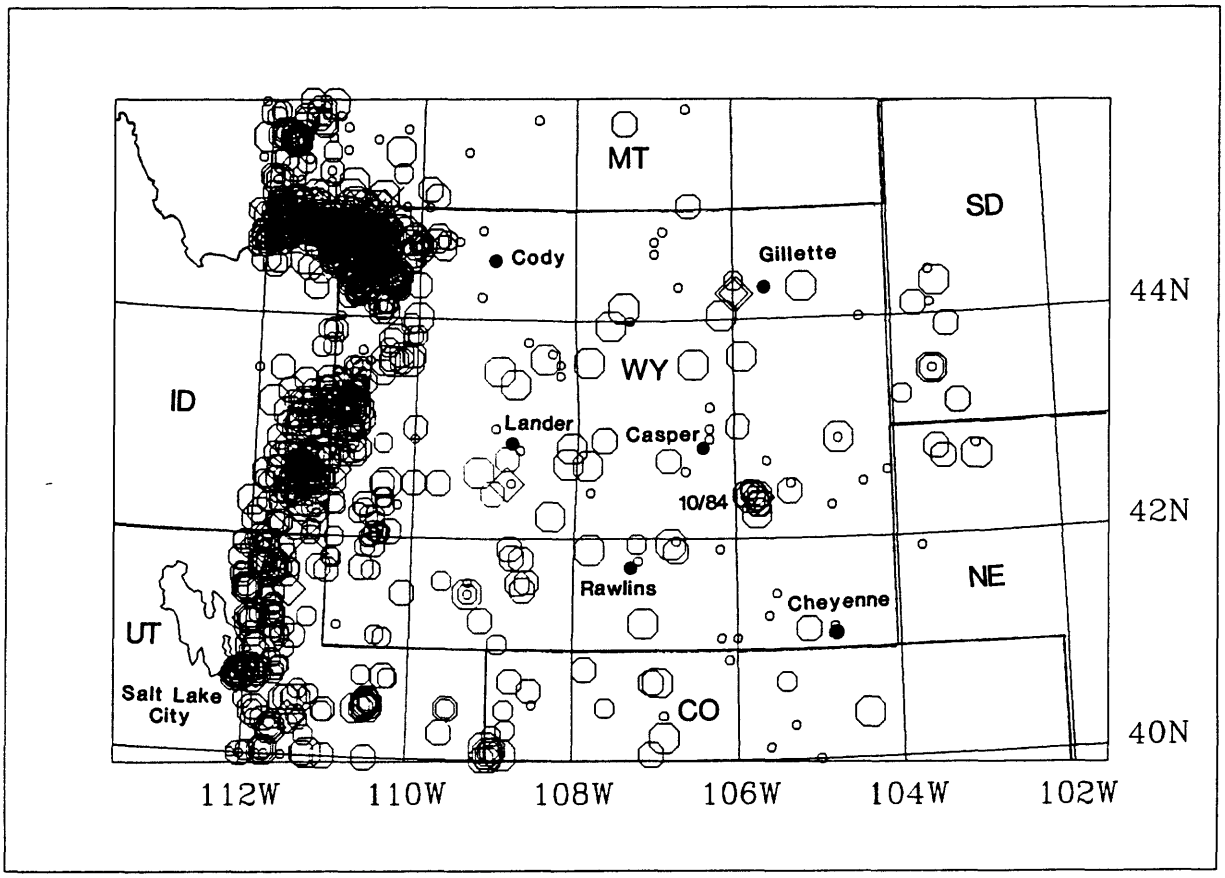

Figure 1. (a) Epicenter map of Wyoming seismicity through 1987 (from U.S. Geological Survey NEIC Earthquake Data Base System compiled by Glen Reagor and Carl Stover). Instrumental epicenters are indicated by appropriate magnitude symbol; macroseismic epicenters denoted by small open circles; 1984 Laramie Mountains sequence is cluster of epicenters southeast of Casper.

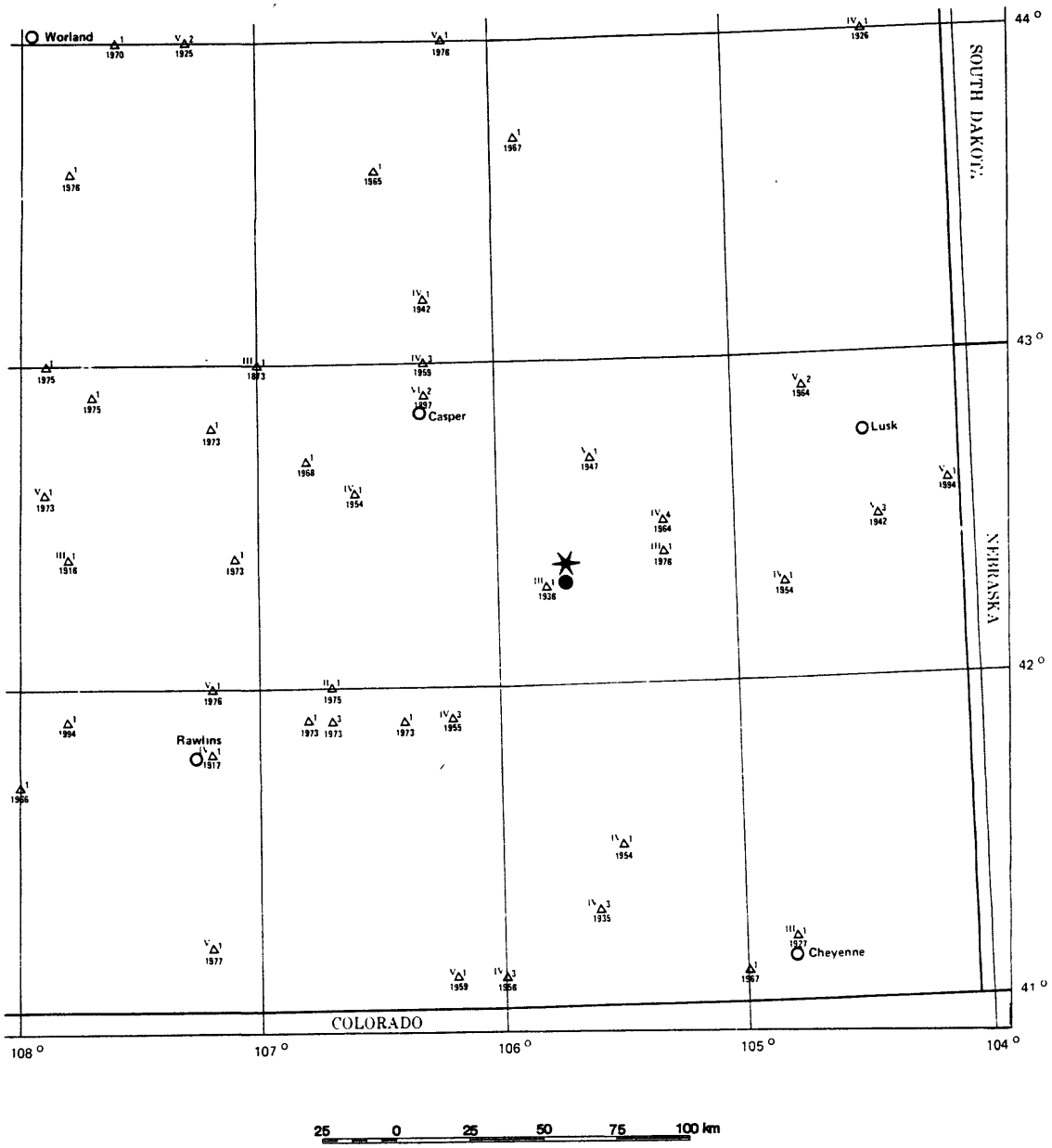

Figure 1. (b) Historical seismicity of southeastern Wyoming through 1981 compiled by Reagor and others (1985). Triangles represent epicenters plotted to nearest 0.1°, number of earthquakes at each location is indicated by number to right of triangle; Roman numeral to left of triangle is maximum intensity (MM) of all earthquakes at that geographic location. Four-digit number below triangle is latest year for which maximum intensity was recorded. Six-pointed star is 1984 main shock epicenter (U.S. Geological Survey, 1984); solid circle is center of aftershocks located by this study.

TABLE 1. — Summary of Wyoming earthquakes, MMIo >/= V, from 1894 (date of first reported earthquake inside the state) to 1990 except for those occurring within the Yellowstone National Park boundaries.

Date (Yr-Mo-Dy)	Time (UTC)	Locality	Lat. (deg N)	Long. (deg W)	Felt Area (sq mi)	Intensity (MMIo)	Magnitude	Remarks	Refer.
1894.06.25	1015	Casper	42.9	106.3	———	V	——	Nearly everyone awakened in Casper; strong shaking on Casper Mtn. (people thrown from their beds).	1,5
1897.11.14	1330	Casper	42.9	106.3	———	VI – VII	——	More violent than 1894 shock; Casper Grand Hotel damaged (2-4" wide crack in NE corner of brick building from third to first floor; lobby ceiling cracked); rumbling noise heard from SW.	1,5
1910.07.26	0130	Rock Springs	41.5	109.3	———	V	——	Intensity V at Rock Springs; mine shafts disturbed.	1
1922.10.26	0120	Bucknum-Salt Cr area	43.2	106.5	———	V	——	Slight damage at Box C ranch N of Bucknum; intensity V at Bucknum and Salt Creek.	5
1923.03.24-.04.12	0400	Jackson Hole	43.6	110.6	1,500	V	——	Intensity V at Kelly, 13 felt shocks.	1
1925.11.18	0150	N.Central Wyo.	44.6	107.0	3,000	V	——	Strong shaking & rumbling sounds at Big Horn (intensity V).	1
1928.02.13	1400	Owl Creek Mtns (?) near Thermopolis	43.5	108.2	3,000	V	——	Intensity V at Thermopolis, Worland, Owl Creek, Gebo, Crosby, Kirby, and at mine in Copper Mountain.	2,3a
1930.06.12	0915	Salt River Range (?), N of Afton	42.6	111.0	———	VI	——	Minor damage at Grover, strong rumbling sounds; aftershocks felt thru 11/16.	1,3a
1930.07.28	0935	Rock Springs	41.5	109.3	———	V	——	Intensity V at Rock Springs.	2,3a
1931.09.21	0515	Southern Laramie Mtns (?)	41.3 (———	105.5 ———)	* ———	V	——	Intensity V at Laramie, felt by nearly all.	2,3a
1932.01.26	1013	Jackson Hole	43.6	110.8	1,000	V-VI	——	Minor damage at Jackson; intensity V at Kelly, Grovant, and Moran; aftershocks felt at Jackson.	1,3a
1934.11.23	2340	Southern Wind River Range	42.8 (43.0	109.1 109.0)	* 8,000	V	——	Intensity V at Lander; strong at Atlantic City, South Pass City, and Fort Washakie to Dubois.	1,3a
1936.01.15	0440	Jackson Lake (?)	44.0 (———	110.7 ———)	* 1,200	V-VI	——	Cracked two chimneys at South Entrance (VI-?), intensity V at Moran.	1,3b
1942.02.25	1410	Fort Laramie	42.5	104.4	———	V	——	Intensity V at Jay EM and Fort Laramie.	2
1944.10.03	0236	Jackson Hole	43.8 (———	110.5 ———)	* ———	V	——	Intensity V at Moran with rumbling sounds (3 shocks); felt at South Entrance.	2,3c
1948.02.24	0239	Jackson Hole	43.5 (43.5	110.5 111.0)	* 1,500	VI	——	Heavy objects shifted at Moran, no damage (VI-?); intensity V near Kelly.	1
1954.01.20	2050	Medicine Bow Mtns, SW of Laramie	41.1 (41.5	106.0 105.5)	* 2,000	V	——	Intensity V at Laramie, Foxpark, Centennial, Jelm, and Albany; two aftershocks felt at Foxpark and Jelm; strong aftershock at Jelm on Jan. 22 (intensity IV).	3d
1954.02.01	0330	Hot Springs State Park (ESE, near Thermopolis)	43.6 (———	108.1 ———)	* ———	V	——	Intensity V at Big Spring, (Hot Springs State Park); many alarmed at Thermopolis.	2,3d
1959.12.25	1650	Medicine Bow Mtns, SW of Laramie	41.1 (41.1	106.0 106.2)	* ———	V	——	Slight damage at Foxpark; felt by all at Jelm.	1,3e
1963.02.25	1845	Big Horn Ridge (?), N of Lander, E of Wind River Range	43.0 (42.6	108.8 109.2)	* ———	V	4.3	Intensity V at Fort Washakie and Lander; in Lander, loud noises heard from north.	3f

TABLE 1. — Summary of Wyoming earthquakes, 1894 to 1990 — continued

1964.03.28	0300	E Central Wyo NNW of Van Tassell	42.7	104.1	———	V	——	Intensity V at Van Tassell.	2
1964.08.22	0328	E Central Wyo NNE of Keeline	42.9	104.7	1,500	V	4.5	Intensity V at Keeline,Lusk and Lost Springs; aftershock felt at Keeline.	1,2,3g
1972.12.08	1847	Owl Creek, NW of Thermopolis	43.7	108.4	———	V	4.1	Slight damage at Thermopolis; strong at Boysen Peak.	1,2
1973.04.22	0607	Western Granite Mtns (?), NW of Jeffrey City	42.6	107.8	———	V	4.8	Intensity V at Jeffrey City; felt in area from Jeffrey City to Lander.	1,3h
1974.09.19	1536	Central Big Horn Mtns (?) NE of Ten Sleep	44.11	107.38	———	V	4.4	Intensity V at Ten Sleep.	1,2
1976.01.27	1054	East Haystack Mtns (?), N of Rawlins	41.95	107.22	———	V	2.3	Intensity V at Rawlins.	1,2
1976.09.03	0418	Powder River Basin near Pumkin Cr	44.041	106.154	———	V	4.8	Intensity V at Kaycee.	1,2
1982.03.01	1043	NW Salt River Range,S of Alpine	42.99	111.04	———	V	3.6	Intensity V at Freedom.	2
1984.05.29	2018	Powder River Basin, 37 km W of Gillette	44.232	105.965	56,000	V	5.0	Intensity V at Gillette, Linch, and Casper.	3i,4
1984.09.08	0059	Powder River Basin, 30 km W of Gillette	44.240	106.019	68,000	V	5.1	Intensity V at Buffalo, Casper,Kaycee,Linch,and Midwest.	3i,4
1984.10.18	1530	N. Laramie Mtns, Fortymile Flat	42.375	105.720	287,000	VI	5.4	Minor damage (intensity VI) at Casper,Douglas,Guernsey, Hanna,Lusk,McFadden,Medicine Bow,Rock River,and Shirley Basin; numerous intensity V effects in SE Wyo.,NE Colo., W Neb. and SW So. Dak..	3i,4
1984.11.03	0930	Southern Wind River Range	42.494	108.854	———	VI	5.0	Minor damage (intensity VI) at Lander;intensity V at Fort Washakie, South Pass City, and Superior.	3i,4

* Revised epicentral coordinates, this report; previous coordinates in parantheses.

References:

1. Coffman, J. L., von Hake, C. A., and Stover, C. W. (ed's), 1982.

2. Reagor, G., and Stover, C. W., 1990.

3a. U. S. Department of Commerce, Enviornmental Science Services Administration, 1968.

3b. U. S. Department of Commerce, Enviornmental Science Services Administration, 1969.

3c. U. S. Department of Commerce, compiled by R. R. Bodle, 1946.

3d. U. S. Department of Commerce, compiled by L. M. Murphy and W. K. Cloud, 1956.

3e. U. S. Department of Commerce, compiled by R. A. Eppley and W. K. Cloud, 1961.

3f. U. S. Department of Commerce, compiled by C. A. von Hake and W. K. Cloud, 1965.

3g. U. S. Department of Commerce, Enviornmental Science Services Administration, compiled by C. A. von Hake and W. K. Cloud, 1966.

3h. U. S. Department of Commerce and U. S. Department of Interior, 1975.

3i. Stover, C. W., 1988.

4. Stover, C. W., 1985.

5. Mokler, A. J., 1923.

evaluation of local geologic lineaments and how this current seismicity and possible predecessors might relate to any such features. In the following discussion, we first review the parameters of the main shock, the results of an intensity survey, and the regional geologic setting. Next, the principal portion of this paper addresses in detail the aftershock locations, the aftershock focal mechanism solutions, and field study of local geologic lineations.

MAIN SHOCK AND LARGEST AFTERSHOCKS

The October 1984 Preliminary Determination of Epicenters (PDE) (U.S. Geological Survey, 1984) gives the following parameters for the main shock as computed by (1) the National Earthquake Information Center (NEIC) and (2) Harvard University (method of Dziewonski and others, 1981):

(1)	NEIC			
	Latitude:	42.375°N	Depth:	33 km (fixed)
	Longitude:	105.720°W	Origin Time:	$15^h30^m23.0^s$UTC
	Magnitude:	5.4 (m_b), 5.5 (M_L), 5.1 (M_s)		
(2)	Harvard			
	Latitude:	42.42°N.	Depth:	21.9 km
	Longitude:	105.21°W.	Origin Time:	$15^h30^m28.4^s$
	M_0:	1.1 X 10^{24} dyne-cm		

Location and magnitude parameters for the six largest aftershocks (see table 2) are also taken from the October 1984 PDE. They are included here for completeness and for comparisons with the regional locations of the NEIC and locations determined by data from our local aftershock network.

Readings from 146 stations were used to determine the main shock hypocenter. The closest station was Black Hills, South Dakota (RSSD), 2.13 deg. (~235 km) from the earthquake source. An apparent 6 km latitude offset (north bias; e.g., see fig. 1b) is observed for the NEIC coordinates compared against the tight clustered group of aftershock epicenters (refer to Aftershock Investigation herein). If it is assumed that the main shock occurred within or very close to the aftershock volume, NEIC's final hypocenter is remarkably good considering the unknown complexities in regional crustal velocities and long distance to the nearest seismograph.

TABLE 2.--Largest aftershocks of the 1984 Laramie Mountains, Wyoming, earthquake (from U.S. Geological Survey, 1984)

Date: 18 Oct 84
Latitude: 42.365°N
Longitude: 105.805°W
Depth: 33 km
Origin time: $15^h57^m37.3^s$ UTC

M_L: 4.2 (GOL)
m_b: 4.5

Date: 18 Oct 84
Latitude: 42.412°N
Longitude: 105.767°W
Depth: 33 km
Origin time: $17^h38^m27.4^s$ UTC

M_L: 3.8 (GOL)

Date: 19 Oct 84
Latitude: 42.41°N
Longitude: 105.77°W
Depth: 33 km
Origin time: $16^h29^m04.4^s$ UTC

M_L: 3.3 (NEIS)

Date: 20 Oct 84
Latitude: 42.40°N
Longitude: 105.8°W
Depth: 33 km
Origin time: $11^h51^m08.6^s$ UTC

M_L: 3.5 (NEIS)

Date: 22 Oct 84
Latitude: 42.40°N
Longitude: 105.88°W
Depth: 33 km
Origin time: $11^h17^m56.3^s$ UTC

M_L: 3.1 (NEIS)

Date: 24 Oct 84
Latitude: 42.322°N
Longitude: 105.717°W
Depth: 33 km
Origin time: $09^h03^m54.7^s$ UTC

M_L: 3.2 (NEIS)

(Note: The 24 October aftershock was relocated by NEIC using results from the aftershock network data; 33 km depths are fixed)

INTENSITY SURVEY

Stover (1985) compiled intensity data obtained from several hundred questionnaires returned by postmasters and police departments within a 400 km radius of the earthquake epicenter. He also included supplemental information gathered by a canvass of selected fire departments and from newspaper reports. Results are shown by the isoseismal map, fig. 2, indicting a small zone of MMI_0 = VI. A summary of the more important intensity observations noted by Stover for the earthquake include:

1. A felt area of 287,000 km^2 that covered parts of seven states. The Laramie Mountains event was felt over an area 2 - 5 times greater than other earthquakes of similar magnitudes in the surrounding region. For example, the m_b = 5.3 Denver earthquake of 9 August 1967 had a felt area of 52,000 km^2 (Herrmann and others, 1981) and the m_b = 5.1 Gillette, Wyoming earthquake of 8 September 1984 had a felt area of 68,000 km^2 (Stover, 1985).
2. No major damage--the most severe was cracks in the exterior brick walls of the Douglas City Hall and the public school in Medicine Bow; also some broken underground pipes in Casper and Shirley Basin. Cracked chimneys and/or cracked exterior brick or cinderblock were observed at Casper, Douglas, Guernsey, Hanna, Lusk, McFadden, Rock River, and Shirley Basin.
3. An unusual report of earthquake damage from Golden, Colorado, about 300 km south of the epicenter. Foundation failure, numerous wall cracks, and a gas leak occurred in a five-story condominium in south Golden as a result of the moderately strong ground shaking.

AFTERSHOCK INVESTIGATION

Field procedure. Station L1, the first seismograph in our aftershock monitoring network (see fig. 3), became operational 24 hours following the main shock. Initially, stations were located to surround the preliminary main shock epicenter about 10 km north of Marshall (for reference, station L1 was sited roughly 1 km northwest of Marshall). Because the aftershocks had depths of more than 20 km, *S-P* time intervals on the early records did not clearly indicate that our initial station distribution was actually centered northwest of the true source zone. After 20 October, the network was reconfigured more to the southeast based on computer-located aftershock hypocenters determined in the field. An optimum distribution of stations was operating by 1400 (UTC) 22 October, some 4 days after the main shock, from which we obtained arrival times to calculate the 47 aftershock hypocenters listed in table 3. Thus, the events being studied are "late" in the aftershock sequence.

Our final network consisted of 16 single, vertical-component, analog recording (smoked paper) seismographs and seven three-component digital systems co-sited with some of the analog units (table 4 lists station coordinates and recording periods). The digital seismograms provided *S*-wave arrival-time data from the horizontal components for this paper; their full analysis will be presented in a subsequent study. Field operations continued for 11 days during which time snow was on the ground over much of the area. In the higher elevations, night time temperatures fell as low as -18°F, but fortunately, very little data were lost as a result of equipment malfunctions caused by the cold weather.

Records and recorder batteries were changed at 24 hour intervals and time corrections checked by comparing the recorder clocks against time standards set by a satellite time code (UTC) receiver. After the clocks became acclimated (~49 hours), their drifts usually did not exceed 25 ms/day.

Data analysis. Crustal thickness in the vicinity of the earthquake is thought to be about 40 km (Prodehl and Pakiser, 1980; Allmendinger and others, 1982). A simple one-layer (40 km thick) over a half-space velocity structure was assumed for the HYPOELLIPSE locations (see bottom of table 3). As a first approximation, we applied a *P*-wave velocity of 6.2 km/sec (based on results of Jackson and Pakiser, 1965 and Prodehl and Pakiser, 1980) with V_p/V_s = 1.70, determined from the Wadati plot derived from network data and shown in figure 4. Quality factors (SQD, table 3) for aftershock hypocenters are A/A except for No. 11 (A/B) indicating that the error statistics and station distribution are mostly graded as excellent. Averages of the

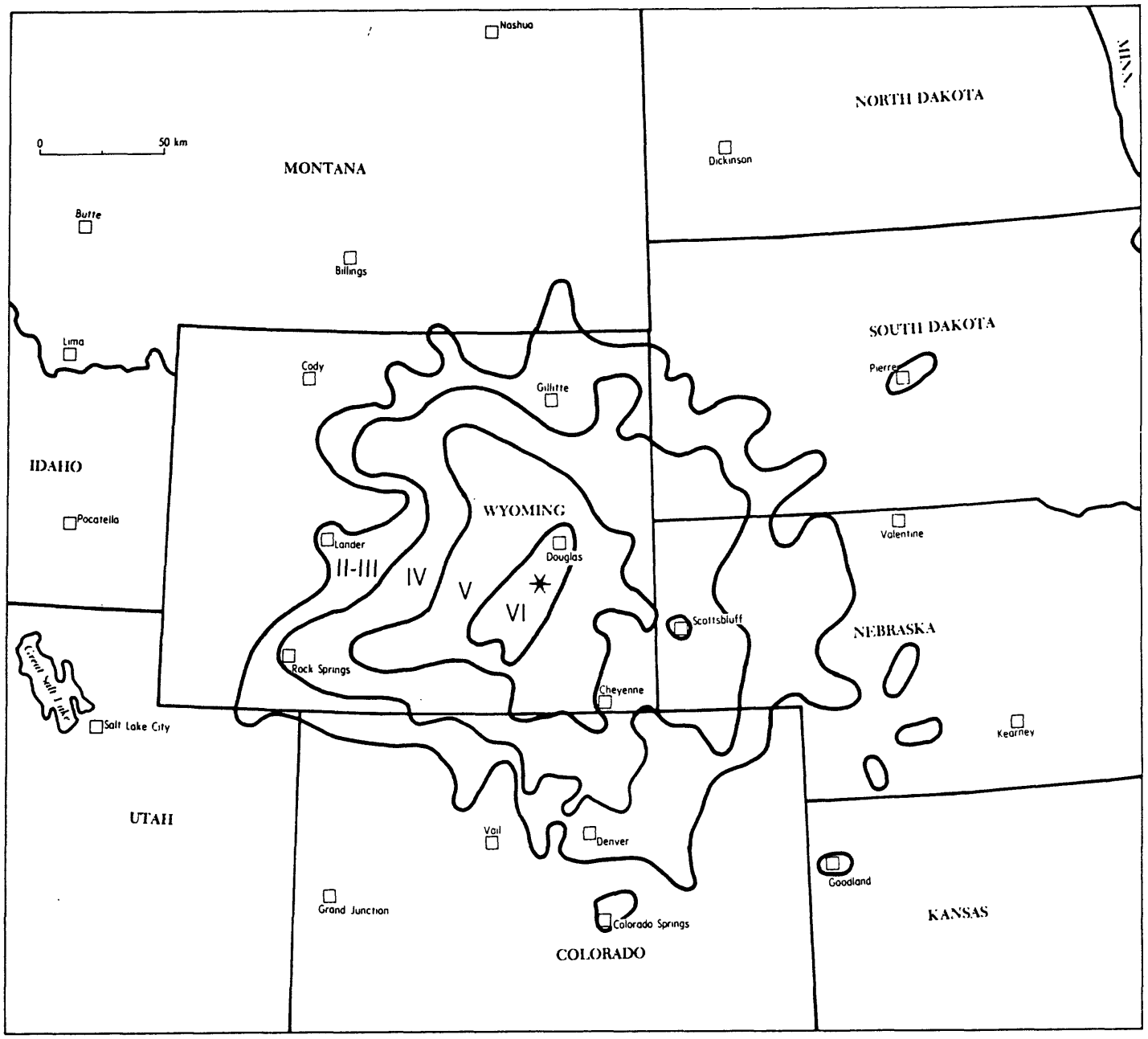

Figure 2. Isoseismal map for 18 October 1984 Laramie Mountains, Wyoming, earthquake from Stover (1985). Star is main shock epicenter.

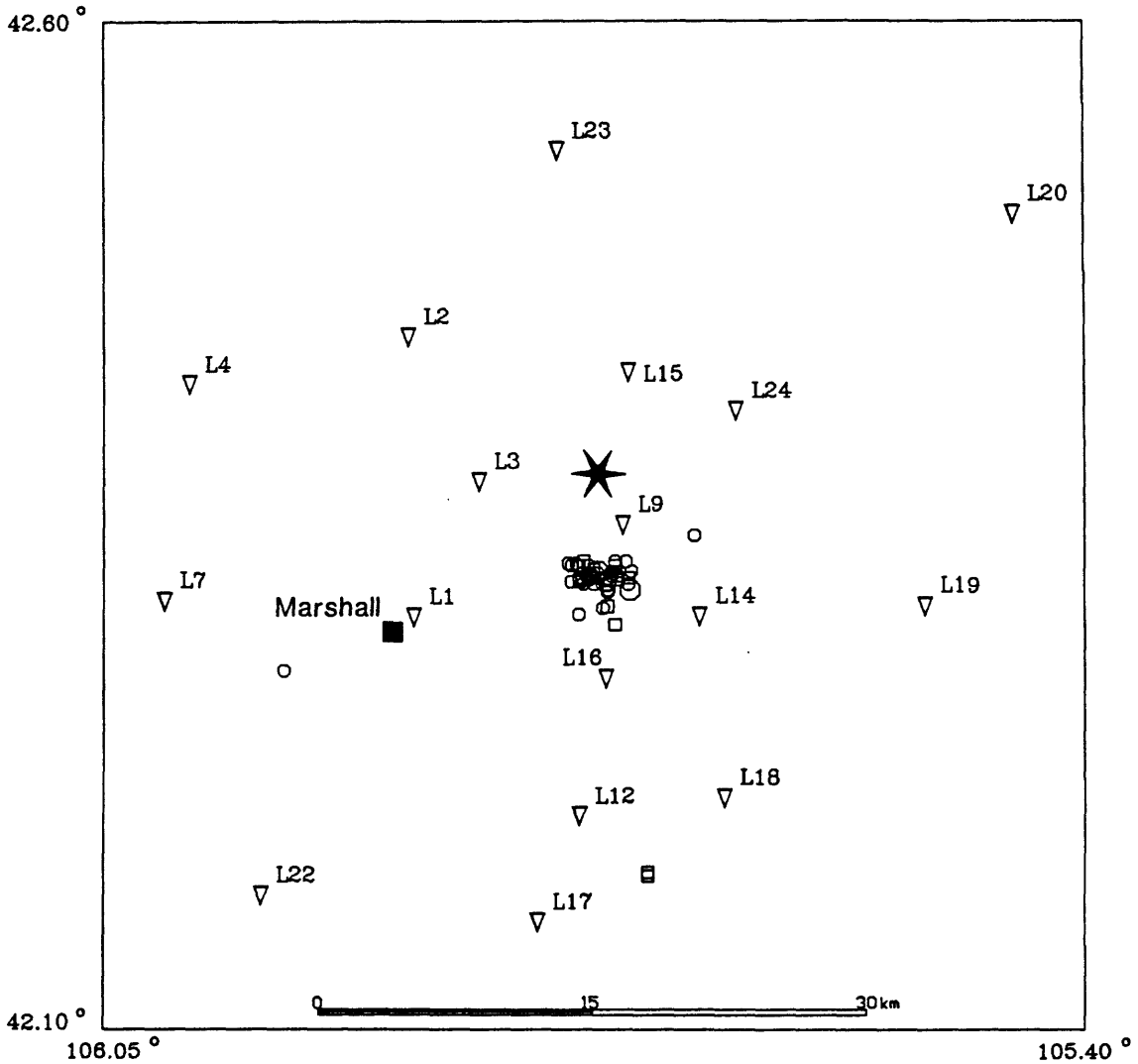

Figure 3. Aftershock epicenter map showing distribution of temporary network stations (triangles with alphanumeric indicator). Main shock epicenter (six-pointed star) is from U.S. Geological Survey (1984); aftershock epicenter symbols are keyed to magnitude (small square is M_d < 2.0, small circle is 2.0 ≤ M_d < 3.0, octagon is M_d ≥ 3.0). Event (small circle) southwest of Marshall (solid square) is in east Shirley Basin and probably not related to the aftershock sequence; two events (small squares) southwest of L12 are quarry blasts.

TABLE 3. —— Summary of aftershock hypocenter parameters computed by HYPOELLIPSE (Lahr, 1984) using locally recorded data

	EQ NO	DATE (YMD)	ORGN TIME (UTC)	LAT (deg)	LONG (deg)	DEPTH (km)	1 DMIN (km)	2 MAG (Md)	3 NO	4 GAP (deg)	5 RMS (sec)	6 ERZ (km)	7 AZ1 (deg)	8 ERH1 (km)	9 AZ2 (deg)	10 ERH2 (km)	11 SQD
	1	841022	1846 46.78	42.318N	105.716W	22.74	4.8	2.766	15	70	0.03	0.31	12.	0.19	-78.	0.17	A/A
	2	841022	1852 19.64	42.345N	105.658W	24.62	4.4	2.395	15	66	0.05	0.44	-1.	0.28	-91.	0.26	A/A
	3	841022	2007 50.98	42.325N	105.709W	23.53	5.1	2.475	16	48	0.03	0.26	-25.	0.16	-115.	0.14	A/A
•	4	841022	2220 57.27	42.381N	106.176W	5.24	15.8	2.247	15	293	0.07	2.26	-67.	0.91	23.	0.49	B/D
	5	841022	2316 30.65	42.323N	105.709W	21.25	5.0	1.997	16	48	0.03	0.30	-25.	0.17	-115.	0.16	A/A
	6	841022	2323 37.06	42.325N	105.726W	21.91	5.7	2.421	16	48	0.04	0.35	-20.	0.20	-110.	0.18	A/A
	7	841023	0015 34.45	42.332N	105.711W	22.04	5.6	2.201	16	49	0.05	0.47	-20.	0.27	-110.	0.25	A/A
	8	841023	0534 53.89	42.322N	105.746W	22.66	5.6	2.137	16	49	0.03	0.32	-19.	0.18	-109.	0.16	A/A
	9	841023	0549 56.66	42.332N	105.704W	23.77	5.1	2.271	16	50	0.02	0.22	-22.	0.14	-112.	0.12	A/A
	10	841023	0848 07.03	42.330N	105.735W	22.50	6.4	1.776	15	51	0.04	0.33	-22.	0.19	-112.	0.17	A/A
	11	841023	0934 53.74	42.277N	105.933W	20.26	8.0	2.128	15	117	0.03	0.42	-112.	0.19	-22.	0.19	A/B
	12	841023	1049 27.04	42.327N	105.712W	21.80	5.4	2.499	15	48	0.04	0.35	-28.	0.21	-118.	0.19	A/A
	13	841023	1143 05.13	42.321N	105.725W	23.17	5.2	2.165	14	46	0.03	0.24	-19.	0.15	-109.	0.13	A/A
	14	841023	1301 46.76	42.327N	105.708W	21.90	4.5	2.244	14	50	0.03	0.24	-21.	0.16	-111.	0.13	A/A
	15	841023	1333 18.73	42.324N	105.702W	22.06	4.5	1.950	15	49	0.04	0.41	-19.	0.20	-109.	0.19	A/A
	16	841023	1458 15.84	42.309N	105.719W	24.78	4.7	2.508	15	53	0.03	0.33	-20.	0.21	-110.	0.18	A/A
	17	841023	1543 34.70	42.321N	105.732W	21.93	5.4	2.692	16	47	0.04	0.34	-20.	0.19	-110.	0.18	A/A
	18	841023	1944 21.69	42.325N	105.729W	20.34	6.6	2.842	15	45	0.05	0.47	-31.	0.23	-121.	0.21	A/A
	19	841023	2223 24.41	42.318N	105.708W	23.30	4.1	3.035	16	48	0.03	0.28	-46.	0.17	44.	0.15	A/A
	20	841024	0203 32.67	42.321N	105.702W	23.24	4.4	2.006	17	48	0.05	0.45	-63.	0.26	27.	0.24	A/A
	21	841024	0408 54.10	42.324N	105.733W	22.17	5.7	2.383	17	45	0.03	0.29	-63.	0.16	27.	0.15	A/A
	22	841024	0719 32.69	42.326N	105.722W	22.29	5.8	3.065	17	47	0.04	0.31	-64.	0.18	26.	0.16	A/A
	23	841024	0832 13.66	42.330N	105.736W	22.80	6.4	1.995	17	46	0.04	0.34	-62.	0.19	28.	0.17	A/A
	24	841024	0903 54.75	42.322N	105.717W	22.07	5.3	3.250	17	46	0.03	0.24	-64.	0.14	26.	0.13	A/A
	25	841024	1439 26.89	42.325N	105.727W	22.12	5.7	2.047	16	46	0.03	0.30	-61.	0.17	29.	0.15	A/A
	26	841024	1538 58.63	42.324N	105.735W	22.10	5.8	2.154	17	45	0.03	0.29	-63.	0.16	27.	0.15	A/A
	27	841024	1813 03.96	42.331N	105.742W	22.38	6.6	2.729	17	41	0.04	0.32	-62.	0.17	28.	0.16	A/A
	28	841025	0834 11.69	42.330N	105.746W	22.10	6.5	2.165	17	44	0.04	0.35	-63.	0.19	27.	0.18	A/A
	29	841025	0817 41.17	42.329N	105.729W	22.18	6.2	2.154	17	46	0.03	0.29	-64.	0.16	26.	0.15	A/A
	30	841025	0927 26.88	42.324N	105.722W	22.61	5.5	1.752	17	46	0.03	0.26	-63.	0.15	27.	0.14	A/A
	31	841025	1233 16.32	42.306N	105.734W	25.61	5.5	2.412	18	51	0.04	0.34	-15.	0.20	-105.	0.17	A/A
••	32	841025	1434 05.03	42.174N	105.688W	0.03	6.2	1.862	17	204	0.10	30.31	-32.	0.43	-122.	0.23	C/D
••	33	841025	1452 07.52	42.174N	105.688W	0.51	6.2	1.538	12	204	0.09	7.53	-36.	0.56	-126.	0.32	C/D
	34	841026	1356 44.41	42.323N	105.732W	21.33	5.6	1.800	16	57	0.04	0.44	-111.	0.25	-21.	0.21	A/A
	35	841026	1358 39.49	42.331N	105.737W	22.26	6.5	2.188	17	46	0.04	0.32	-63.	0.17	27.	0.16	A/A
	36	841026	1429 16.98	42.324N	105.727W	22.53	5.5	2.016	17	46	0.04	0.34	-63.	0.19	27.	0.18	A/A
	37	841027	1404 24.52	42.325N	105.713W	23.29	5.4	2.348	17	48	0.02	0.20	-63.	0.12	27.	0.11	A/A
	38	841027	1535 22.28	42.330N	105.710W	21.37	5.4	1.995	17	49	0.04	0.34	-67.	0.19	23.	0.18	A/A
	39	841027	2055 08.34	42.326N	105.717W	22.92	5.1	1.646	17	46	0.04	0.34	-62.	0.19	28.	0.17	A/A
	40	841027	2134 14.19	42.325N	105.721W	21.35	5.7	2.250	17	47	0.03	0.29	-65.	0.16	25.	0.15	A/A
	41	841027	2156 08.56	42.326N	105.707W	21.66	5.0	2.251	17	49	0.02	0.19	-66.	0.11	24.	0.10	A/A
	42	841028	0149 24.72	42.310N	105.715W	23.00	4.6	1.992	17	53	0.02	0.21	-60.	0.12	30.	0.11	A/A
	43	841028	0428 33.01	42.332N	105.731W	22.64	6.5	1.168	17	47	0.03	0.29	-63.	0.16	27.	0.15	A/A
	44	841028	0443 13.95	42.328N	105.725W	21.81	6.0	1.957	17	47	0.03	0.24	-65.	0.13	25.	0.12	A/A
	45	841028	0516 51.29	42.321N	105.735W	22.15	5.5	1.641	17	44	0.03	0.25	-62.	0.13	28.	0.12	A/A
	46	841028	0951 12.43	42.301N	105.710W	24.03	4.7	1.467	17	61	0.02	0.20	-58.	0.12	32.	0.10	A/A
	47	841028	1352 17.51	42.323N	105.727W	21.19	5.5	2.505	17	45	0.03	0.28	-65.	0.15	25.	0.14	A/A
	48	841028	1600 58.31	42.323N	105.716W	20.75	5.4	2.695	17	47	0.04	0.37	-66.	0.21	24.	0.19	A/A
	49	841028	1749 46.56	42.318N	105.715W	22.55	4.8	2.385	17	46	0.02	0.21	-63.	0.12	27.	0.11	A/A
	50	841028	1928 01.47	42.317N	105.715W	22.72	4.7	2.213	18	46	0.04	0.32	-66.	0.18	34.	0.16	A/A
		• • AVERAGES • •				22.42	5.5	2.24	16.4	50.	0.03	0.31	-49.	0.18	-24.	0.16	

Note — Average values computed only for aftershocks
No. of aftershocks = 47
• Regional event
•• Quarry blast

1 —Distance to closest seismograph station.
2 —Local magnitude estimate based on signal duration (coda length) of earthquake (see Lee and Stewart, 1981).
3 —Number of observations (P and S) used to compute hypocentral solution.
4 —Largest azimuthal separation, in degrees, between stations as viewed from the epicenter.
5 —Root mean square errors of travel time residuals.
6–10—Error estimates based on 68% confidence ellipsoid (see Lahr, 1984).
11 —Measures indicating general reliability of hypocentral locations where S is solution quality defined by HYPO71:

S	RMS	ERH	ERZ
A	< 0.15	</= 1.0	</= 2.0
B	< 0.30	</= 2.5	</= 5.0
C	< 0.50	</= 5.0	</= 7.5

Q is a spacer between S and D qualities; D is station distribution quality defined by HYPO71:

D	NO	GAP	DMIN
A	</= 6	</= 90	</= DEPTH or 5 km
B	</= 6	</= 135	</= (2)DEPTH or 10 km
C	</= 6	</= 180	</= 50 km
D	Others		

• • • VELOCITY MODEL • • •

LAYER	P-VELOCITY (km/sec)	DEPTH (km)	THICKNESS (km)	VP/VS
1	6.200	0.000	40.000	1.700
2	8.000	40.000	1000.000	1.700

TABLE 4.--Station coordinates and period of operation

Sta	Coordinates					Period of Operation (1984)				
	Latitude (N)		Longitude (W)		Elev	(From)		(TO)		
	(deg)	(min)	(deg)	(min)	(m)	Date	Time (UTC)	Date	Time (UTC)	Instrument Type
L1	42	18.25	105	50.57	2271	10-19	1552	10-29	1544	Smoked paper, digital
L2	42	26.58	105	50.78	2466	10-19	2146	10-29	1516	Smoked paper
L3	42	22.27	105	48.00	2616	10-19	1740	10-29	1648	Smoked paper, digital
L4	42	25.15	105	59.55	2316	10-19	2045	10-29	1450	Smoked paper, digital
L5	42	13.82	105	56.54	2184	10-19	2335	10-22	1729	Smoked paper
L6	42	20.62	106	05.35	2210	10-19	2338	10-22	1610	Smoked paper
L7	42	18.72	106	00.53	2268	10-19	2335	10-29	1423	Smoked paper
L8	42	26.81	106	05.76	2335	10-20	1632	10-21	1615	Smoked paper
L9	42	21.00	105	42.28	2301	10-20	1706	10-29	1746	Smoked paper
L10	42	16.77	105	42.69	2280	10-20	1836	10-21	1929	Smoked paper
L11	42	29.22	105	58.59	2426	10-20	2109	10-21	1925	Smoked paper
L12	42	12.33	105	43.99	2251	10-20	2310	10-29	1810	Smoked paper, digital
L13	42	09.07	105	44.68	2175	10-20	2357	10-21	2022	Smoked paper
L14	42	18.29	105	39.22	2335	10-21	1851	10-29	1723	Smoked paper
L15	42	25.53	105	42.04	2341	10-21	1929	10-29	1634	Smoked paper, digital
L16	42	16.46	105	42.96	2283	10-21	1951	10-29	1853	Smoked paper
L17	42	09.18	105	45.68	2165	10-21	2045	10-29	1913	Smoked paper
L18	42	12.88	105	38.24	2350	10-21	2131	10-29	1530	Smoked paper, digital
L19	42	18.59	105	30.26	2319	10-22	1711	10-29	1602	Smoked paper
L20	42	30.21	105	26.73	1615	10-22	1842	10-29	1646	Smoked paper
L21	42	07.63	105	37.52	2176	10-22	1852	10-23	2005	Smoked paper
L22	42	09.86	105	56.70	2109	10-22	1916	10-29	1926	Smoked paper
L23	42	32.13	105	44.86	2177	10-23	1813	10-29	1556	Smoked paper, digital
L24	42	24.39	105	37.77	2056	10-27	2017	10-29	1718	Smoked paper

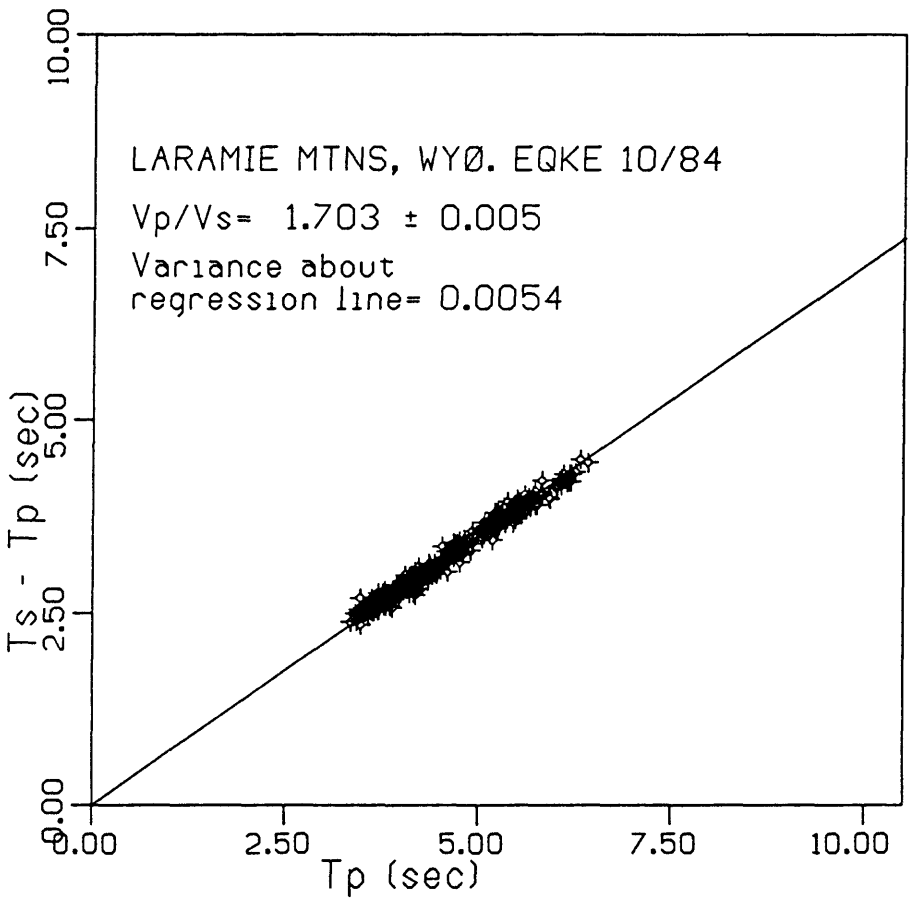

Figure 4. Wadati plot showing travel time of *P*-wave (T_P, sec.) versus travel time of *S*-wave minus travel time of *P*-wave (T_s - T_P, sec.) for 47 aftershocks located with HYPOELLIPSE. Data used are restricted to arrivals with *S* travel time residuals ≤ 0.20 sec. and *P* travel time residuals ≤ 0.10 sec.

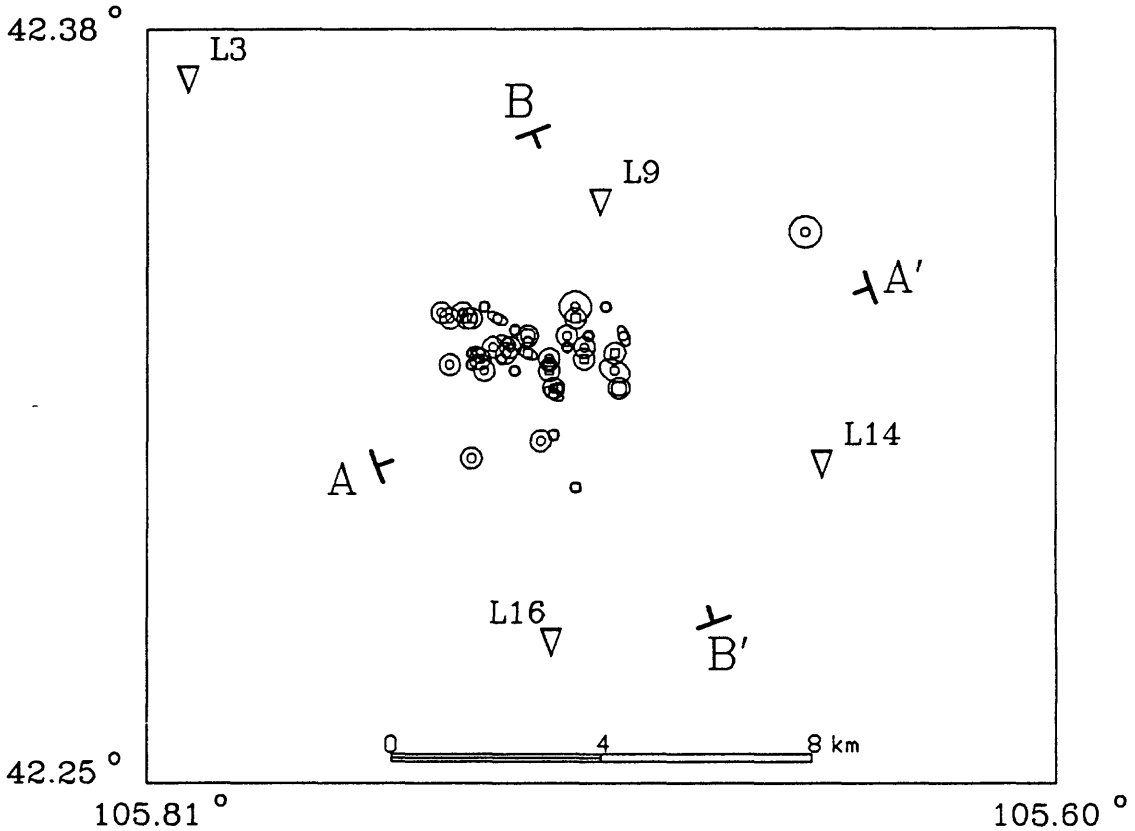

Figure 5. (a) Aftershock epicenters plotted with corresponding error ellipses. A-A' and B-B' are locations of projection planes for (b), other symbols same as figure 3.

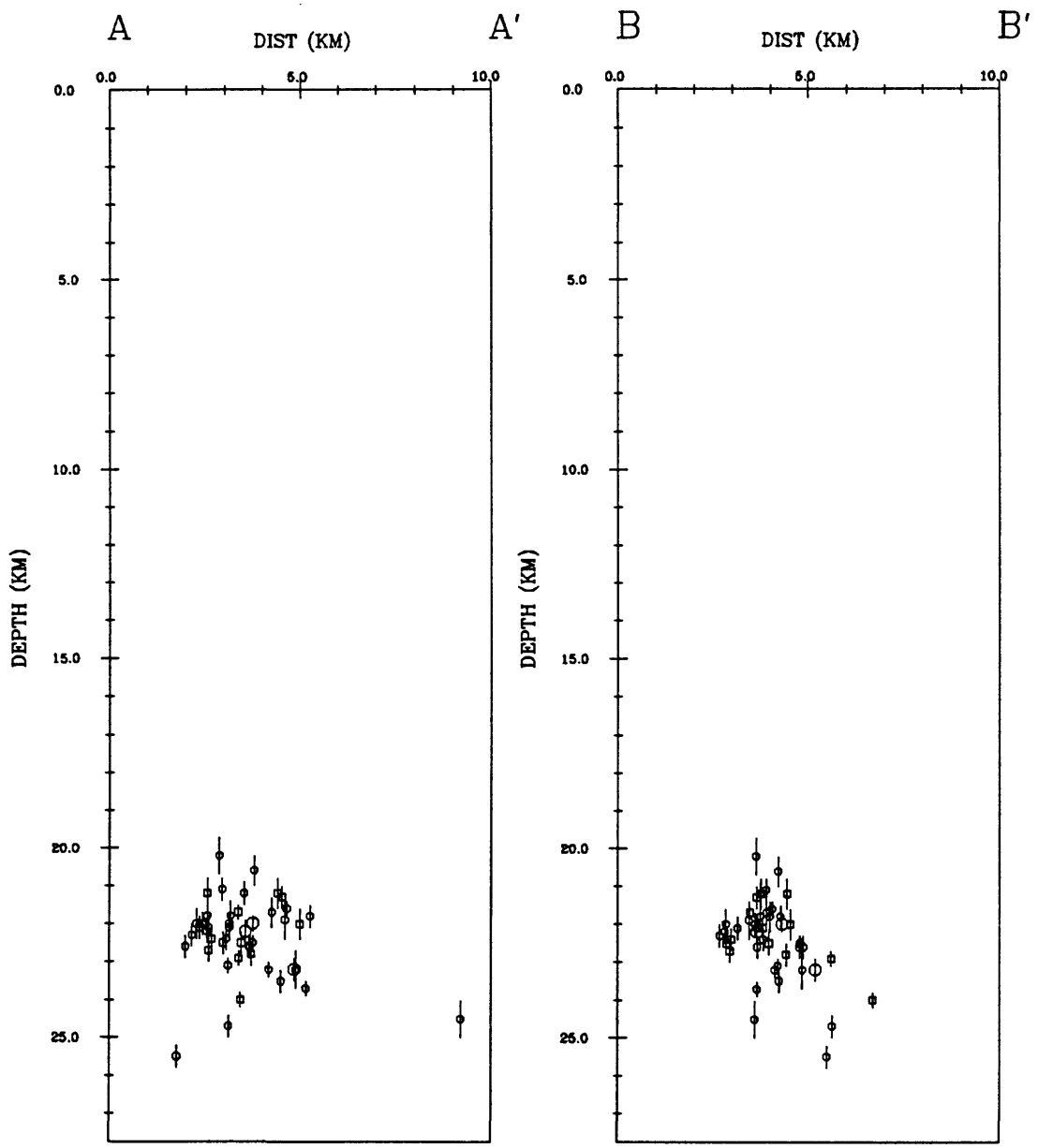

Figure 5 (b) Vertical section plots of hypocenters projected into N. 69° E. (A-A') and N. 26° W. (B-B') planes, same as nodal planes of main shock (fig. 6). Hypocenter symbols same as (a), error ellipses and vertical error bars are based on 68 percent confidence ellipsoid (Lahr, 1984).

68 percent confidence error ellipsoid axes are ERZ = 0.3 km, ERH1 = ERH2 = 0.2 km; average RMS errors of the travel time residuals are 0.03 sec.

Figure 5(a) shows the aftershock epicenters computed by HYPOELLIPSE (Lahr, 1984) with associated error ellipses. Using figures 5a and 5b (epicenters with error ellipses and the distribution of foci with vertical error bars) the aftershock volume appears somewhat cylindrical with dimensions roughly 4 km in diameter and 5-km in height (98 km^3). An isolated aftershock, separated by about 3½ km to the northeast (no. 2, table 3), is not included in the volume calculation. Forty-one foci (87%) concentrate between 21.0 and 23.8 km depth; the average depth for all events (without no. 4 and the two quarry blasts) is 22.5 km.

Applying conservatively large fault dimension approximations (length, L = 4 km; height, H = 5 km) to Aki's (1966) seismic moment relationship for average slip on a fault, $D = \frac{M_o}{\mu A}$ where μ = the shear modulus of the displaced medium (we use 3 X 10^{11} dyne/cm^2), A = fault plane area = (L X H), and D is averaged over the area A, D = 18 cm. From Brune's (1970) equation for stress drop (assuming a circular fault), $\Delta\sigma = \frac{7}{16}\frac{M_o}{r^3}$, using M_o = 1.1 X 10^{24} dyne-cm and r = 2 km, $\Delta\sigma$ = 60 bars.

FOCAL MECHANISM SOLUTIONS

Mainshock. The main shock focal mechanism solution (fig. 6; Gordon, 1987) was constructed primarily from short-period *P*-wave first-motion readings. Indicated displacements for the double-couple solution are predominantly right lateral strike slip to the east-northeast or left lateral strike slip to the north-northwest on steeply dipping (~ 70°-80°) nodal planes. Azimuth of the *T*-axes is N. 23° E. at a low (8.5°) angle of plunge (see fig. 6 for all parameters). Seventy-five first motion data were used including some from stations at epicentral distances of 10° - 20°, i.e., arrivals that may graze or pass through the low velocity layers of the upper mantle. These "low velocity arrivals" may introduce inconsistent or misleading first motions but their overall agreement with the double-couple solution is good.

Aftershocks. First-motion patterns of all 47 located aftershocks were adequate to determine single-event focal mechanism solutions (lower hemisphere, equal-area projections; parameters listed in table 5). Two general classes of mechanisms (normal and strike-slip) were observed. A plot of the distribution of the *P*- and *T*-axes and average *T*-axes direction is shown for four different groupings of those two mechanism types (types 1, 2, 3, and 4 in fig. 7a) accompanied by mechanisms grouped according to type (fig. 7b). Generalized characteristics of the four mechanism types are given in tables 6a, b.

The *T*-axes are the most stable with NE-NNE azimuths and subhorizontal plunges. The *P*-axes, however, are also stable azimuthally, WNW-NW, but exhibit considerable variation in plunge from subhorizontal to subvertical. The normal mode of faulting is, of course, associated with steeper *P*-axes plunges and strike-slip faulting with the shallower *P*-axes.

The mutual occurrence in both space and time of strike-slip and normal faulting in this aftershock sequence suggests that the minimum principal stress stays at a mostly horizontal orientation, but that the intermediate and maximum principal stresses are interchanging plunges between subvertical and subhorizontal. Such interchanges can be expected when the magnitudes of the two stresses involved are very close to the same value. The dominant strikes of the nodal planes are mostly northwest to northeast with some instances of more east-west. That range in strike could be accommodated by reactivation of a pre-existing conjugate set of faults.

A minor degree of temporal association by mechanism type is observed in the aftershocks recorded by our final network configuration (see table 5). In the earlier stages of our monitoring (first 42 hours), normal faulting type 4 mechanisms predominate (11 of the first 20 aftershock locations). Six of the next ten

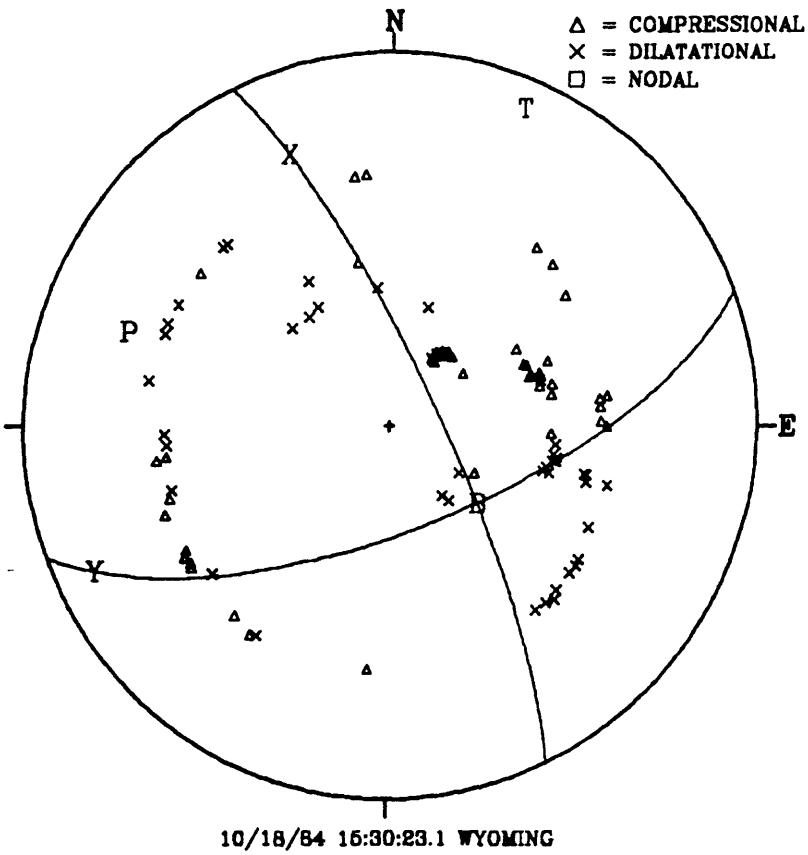

	AZIMUTH	PLUNGE
P axis	289.3	24.7
T axis	23.2	8.5
B axis	130.8	63.7
X axis	338.9	23.5
Y axis	244.0	11.0

334.00	79.00	-24.00
68.88	66.47	-167.99

Figure 6. Main shock focal mechanism solution, lower hemisphere, equal area projection, 65 first-motion readings, 16 inconsistencies. X-nodal plane strikes N. 26° W., dips 79° ENE.; Y-nodal plane strikes N. 69° E., dips 66° SSE.; computed by Gordon (1987).

TABLE 5.–Summary of aftershock focal mechanism solution parameters

Eq	P-axis		T-axis		B-axis		X Nodal Plane			Y Nodal Plane			Mechanism Type			
No	Azimuth	Plunge	Azimuth	Plunge	Azimuth	Plunge	Strike	Dip	Plunge	Strike	Dip	Plunge	1	2	3	4
01	152.0	37.1	57.5	06.0	319.7	52.3	08.0	120.0	24.0	290.6	69.4	212.3		X		
02	139.2	60.0	240.9	06.7	334.6	29.1	-05.0	122.0	55.0	302.1	46.0	227.5				X
03	110.5	27.7	16.4	07.6	272.4	61.1	-30.0	115.0	15.0	246.5	76.4	205.8	X			
05	298.7	25.9	207.4	02.7	111.8	64.0	-20.0	70.0	-17.0	76.0	74.1	-159.2	X			
06	158.8	56.6	56.6	07.4	321.6	32.3	-02.0	133.0	43.0	300.5	60.1	213.9				X
07	150.7	62.5	54.1	03.4	322.4	27.2	-10.0	132.0	52.0	300.6	54.2	235.6				X
08	107.4	05.8	15.3	19.6	213.3	69.5	-27.0	108.0	-10.0	59.9	80.5	-198.3	X			
09	122.8	58.6	238.5	14.8	336.3	26.9	-10.0	115.0	60.0	296.2	38.3	223.0				X
10	164.5	61.8	67.5	03.7	335.5	27.9	04.0	132.0	51.0	313.6	54.7	235.1				X
12	150.3	61.1	52.9	04.0	320.7	28.5	-10.0	132.0	50.0	296.6	55.3	234.5				X
13	145.1	55.4	244.8	06.6	339.2	33.8	02.0	120.0	50.0	302.8	48.4	221.9				X
14	159.5	37.5	53.5	19.7	301.6	45.9	10.0	132.0	15.0	290.2	78.9	223.0		X		
15	149.9	60.4	55.9	02.3	324.7	29.5	-07.0	130.0	50.0	300.4	54.1	232.6				X
16	149.9	58.6	228.5	14.8	326.3	26.9	-20.0	115.0	60.0	286.2	38.3	223.0				X
17	105.9	03.4	14.3	25.2	203.0	64.6	-27.0	110.0	-16.0	57.4	75.0	-200.7	X			
18	162.0	57.4	62.5	12.1	315.5	29.8	-05.0	138.0	42.0	298.8	63.4	236.2				X
19	288.3	50.5	22.8	03.7	115.8	39.3	-36.0	60.0	-43.0	79.0	53.8	-141.7			X	
20	301.7	08.4	33.6	12.7	179.1	74.7	-12.0	93.0	-15.0	77.2	75.0	-183.1	X			
21	160.8	54.2	59.9	07.8	324.4	34.7	03.0	132.0	40.0	302.3	61.5	229.6				X
22	149.9	36.4	55.1	06.6	316.3	52.9	06.0	120.0	23.0	288.0	70.2	212.1		X		
23	326.4	58.2	206.6	17.1	108.1	25.9	-30.0	36.0	-42.0	96.1	68.8	-118.4			X	
24	110.8	28.7	20.7	00.2	290.3	61.3	-28.0	110.0	21.0	249.5	70.3	201.3	X			
25	107.3	23.9	197.7	00.9	289.7	66.1	-30.0	106.0	18.0	245.1	72.7	196.8	X			
26	137.8	35.7	42.6	07.1	302.9	53.4	-06.0	120.0	22.0	275.4	71.1	211.9		X		
27	303.2	73.9	201.9	03.2	111.0	15.7	-52.0	44.0	-67.0	97.5	50.3	-110.7			X	
28	302.9	75.9	206.9	01.7	115.6	14.0	-50.0	45.0	-70.0	102.8	48.4	-108.9			X	
29	290.2	67.5	23.4	01.3	113.9	22.5	92.0	-132.8	-59.0	313.9	50.4	-60.2			X	
30	309.3	68.9	209.2	03.8	117.8	20.7	-40.0	45.0	-60.0	100.8	42.2	-116.6			X	
31	325.3	59.9	208.9	14.4	111.8	25.8	-30.0	38.0	-45.0	98.2	64.2	-118.9			X	
34	144.3	29.4	47.1	12.5	296.6	57.5	02.0	120.0	13.0	278.6	78.8	210.7		X		
35	149.4	65.4	48.0	05.2	315.7	23.9	-18.0	135.0	55.0	297.3	54.6	240.2				X
36	143.5	34.3	47.8	08.3	306.1	54.5	00.00	120.0	20.0	280.3	72.8	211.6		X		
37	307.8	02.7	38.5	14.1	207.2	75.6	-06.0	98.0	-12.0	82.3	78.1	-188.2	X			
38	105.5	27.9	13.6	03.6	276.9	61.9	-34.0	112.0	18.0	242.9	73.4	203.0	X			
39	301.9	77.6	35.1	00.7	125.2	12.3	-43.0	47.0	-73.0	112.8	45.6	-107.4			X	
40	263.9	44.0	01.8	08.2	100.0	44.8	-55.0	67.0	-40.0	53.2	53.7	-151.0			X	
41	156.4	50.6	56.7	07.8	320.5	38.3	02.0	130.0	36.0	297.0	63.2	226.1				X
42	112.7	30.8	15.9	11.2	268.2	56.8	-30.0	120.0	15.0	247.6	77.1	210.9	X			
43	130.4	45.3	227.0	06.5	323.3	44.0	-10.0	115.0	40.0	279.5	54.4	211.3				X
44	156.0	50.1	53.4	10.3	315.2	38.0	00.0	132.0	34.0	294.3	65.5	227.4				X
45	305.2	08.1	38.1	19.7	193.9	68.5	-07.0	98.0	-20.0	80.1	70.2	-188.5	X			
46	134.0	37.0	246.5	23.9	358.3	43.5	06.0	98.0	46.0	284.2	44.6	191.4		X		
47	276.1	41.8	22.4	17.5	129.5	43.1	-36.0	75.0	-45.0	68.5	46.9	-159.3			X	
48	292.7	12.7	202.7	00.1	112.4	77.3	-23.0	81.0	-09.0	68.4	81.1	-170.9	X			
49	265.1	48.1	10.9	13.7	112.1	38.7	-50.0	69.0	-48.0	61.7	46.1	-150.2			X	
50	308.7	63.1	41.1	01.2	131.7	26.9	-25.0	52.0	-55.0	106.3	49.8	-126.3			X	

NOTE: Aftershock numbers indicate relative chronological positions, same as Table 3.

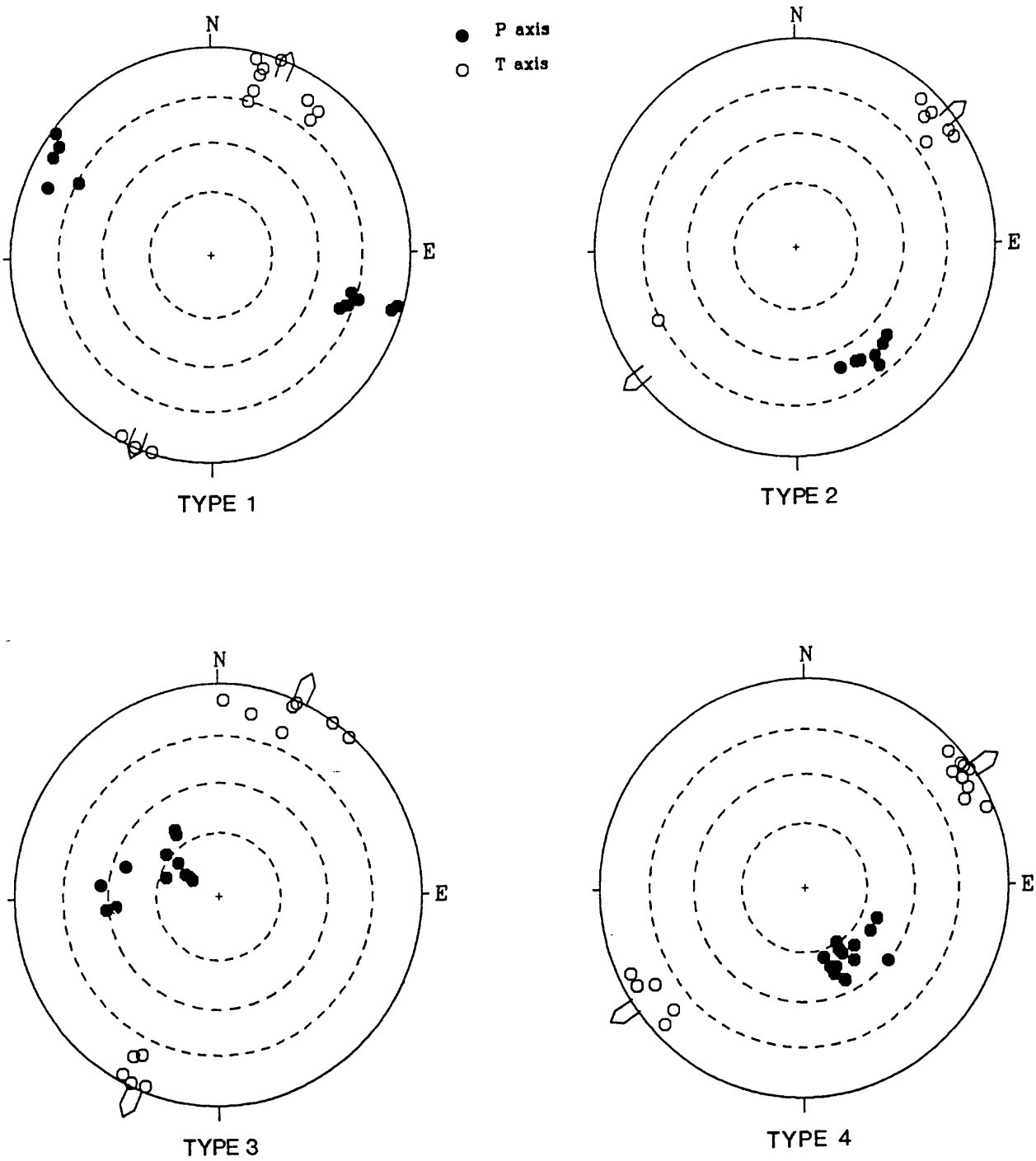

Figure 7. (a) Distribution of *P*- and *T*-axes for types 1, 2, 3, and 4 aftershock focal mechanism solutions plotted on equal area projections. Dashed circles indicate angles of plunge at 25, 45, 65 degree (outer, middle, and inner ring, respectively); pointed symbol denotes average azimuth of *T*-axes.

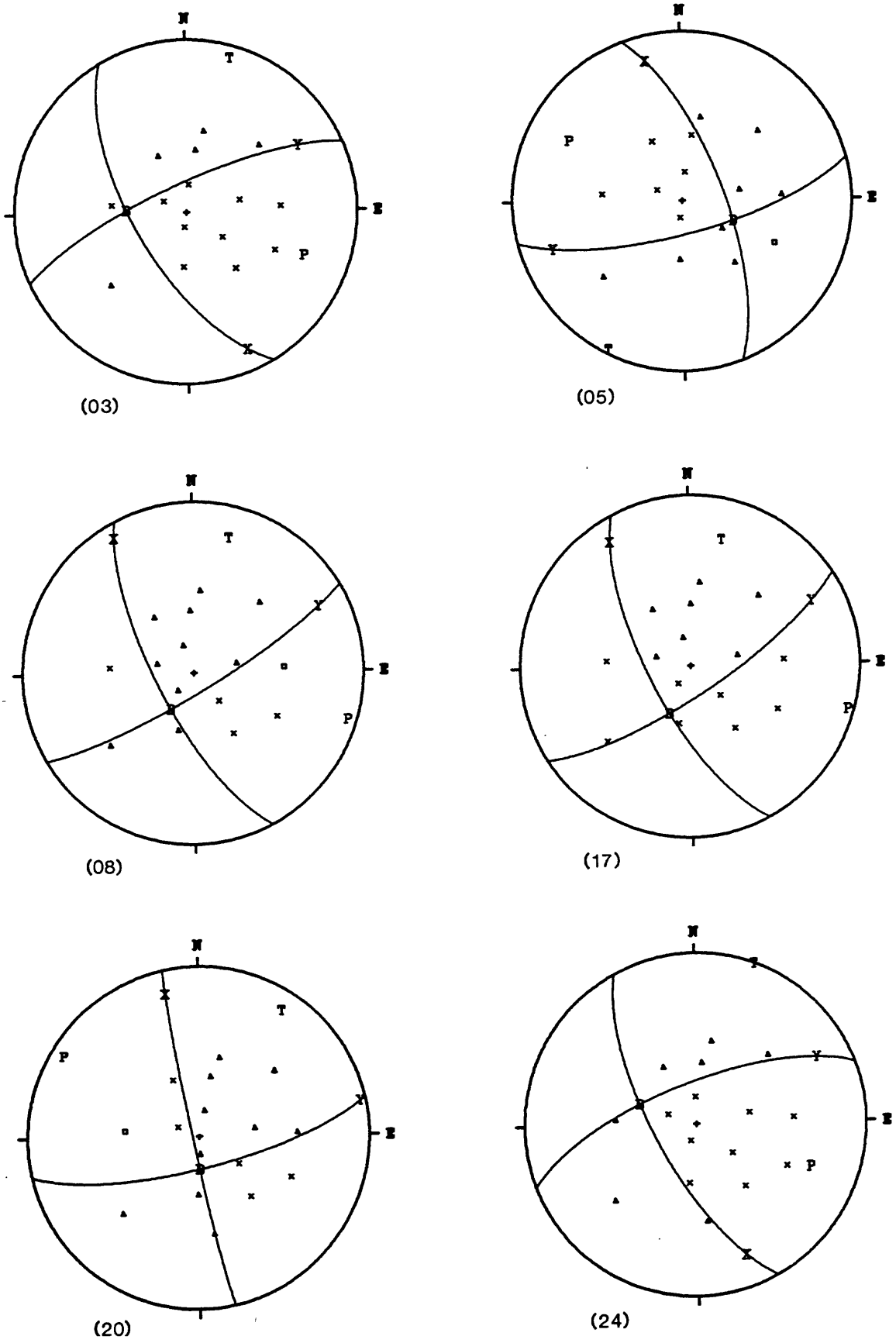

Figure 7. (b) Type 1 aftershock focal mechanism solutions.

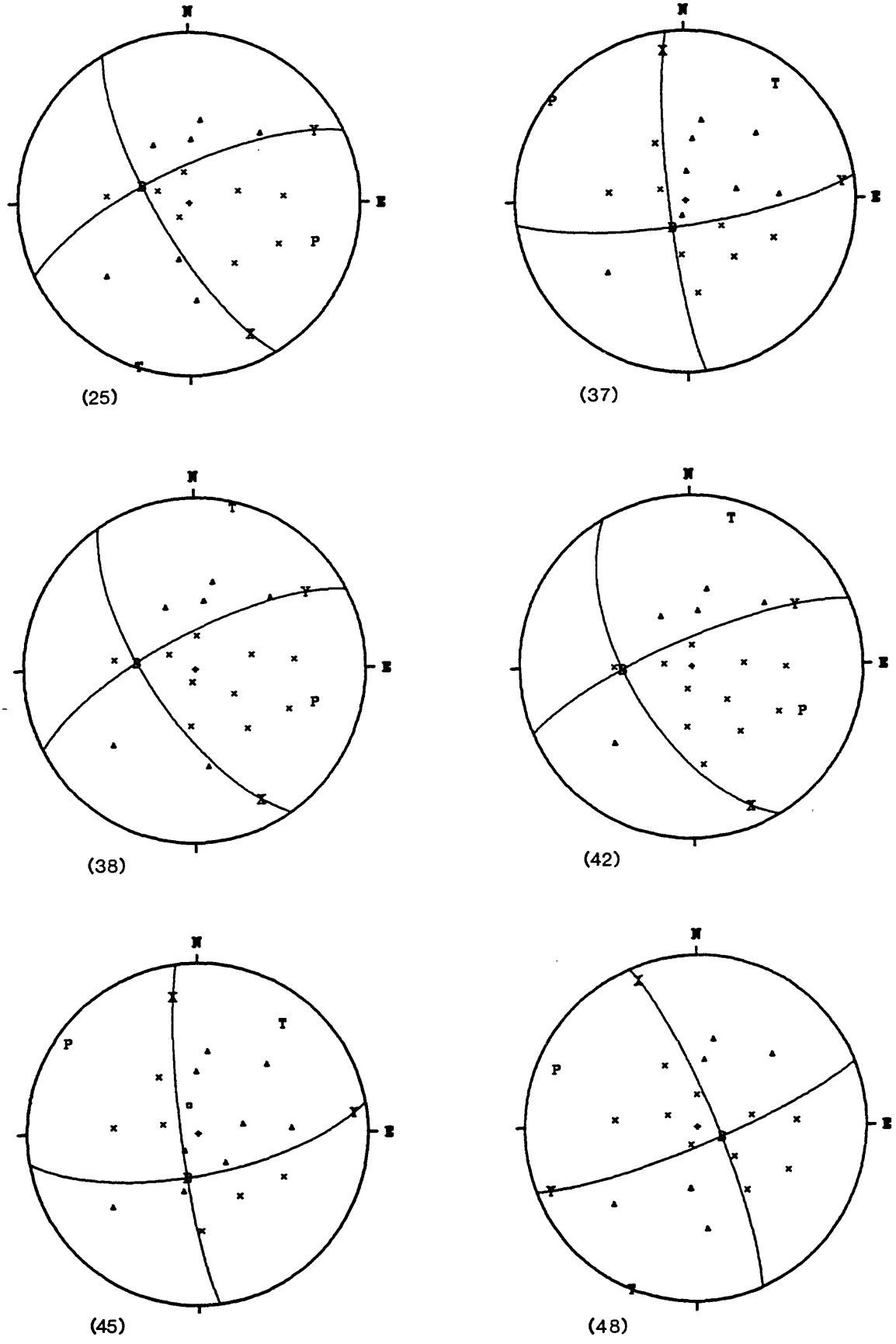

Figure 7. (b) Type 1 aftershock focal mechanism solutions (continued).

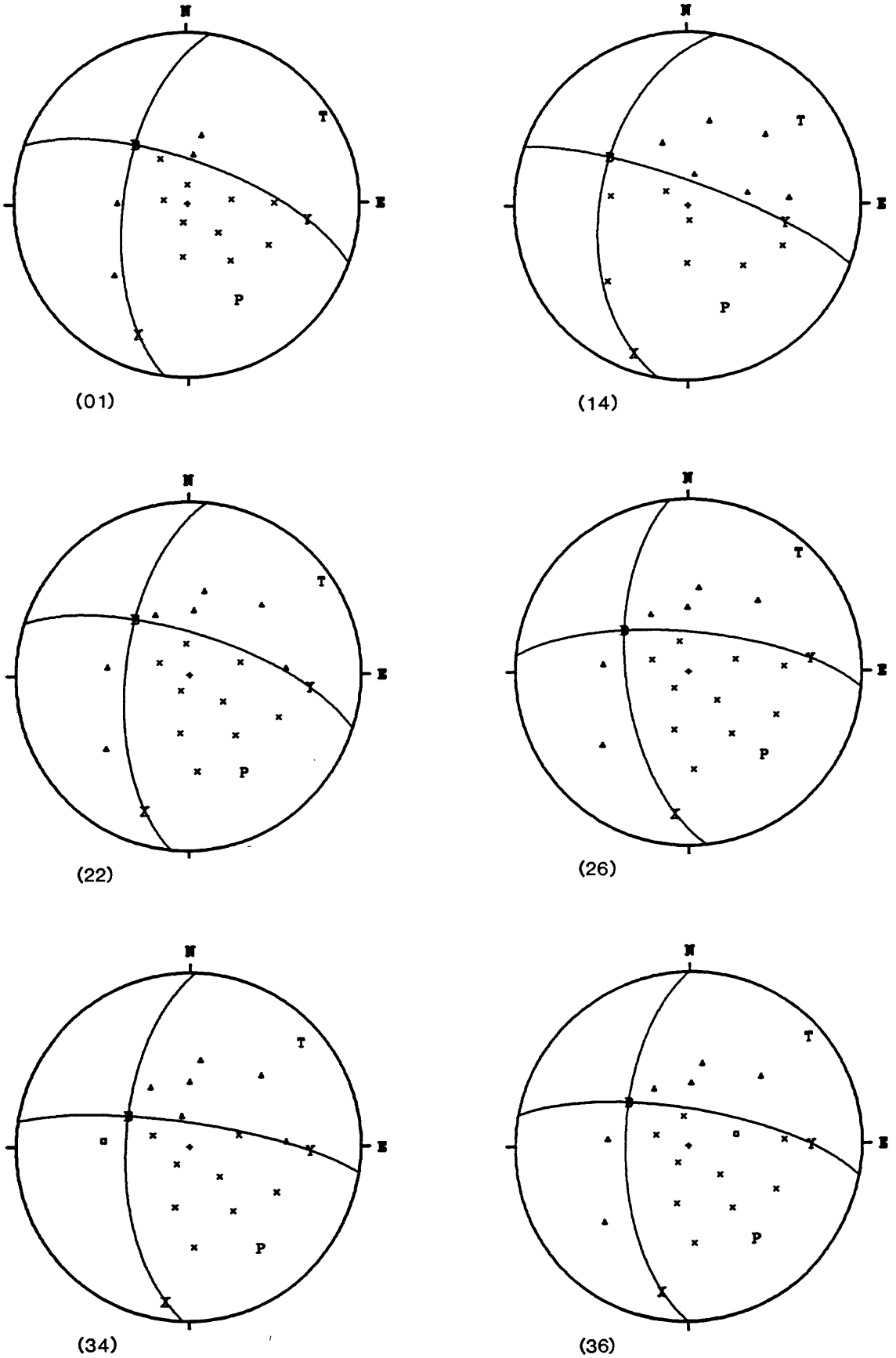

Figure 7. (b) Type 2 aftershock focal mechanism solutions.

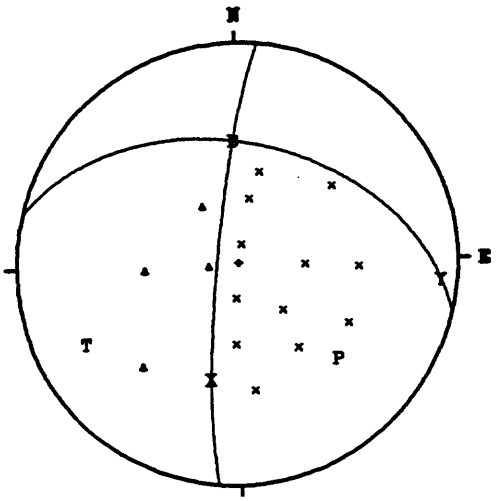

(46)

Figure 7. (b) Type 2 aftershock focal mechanism solution (continued).

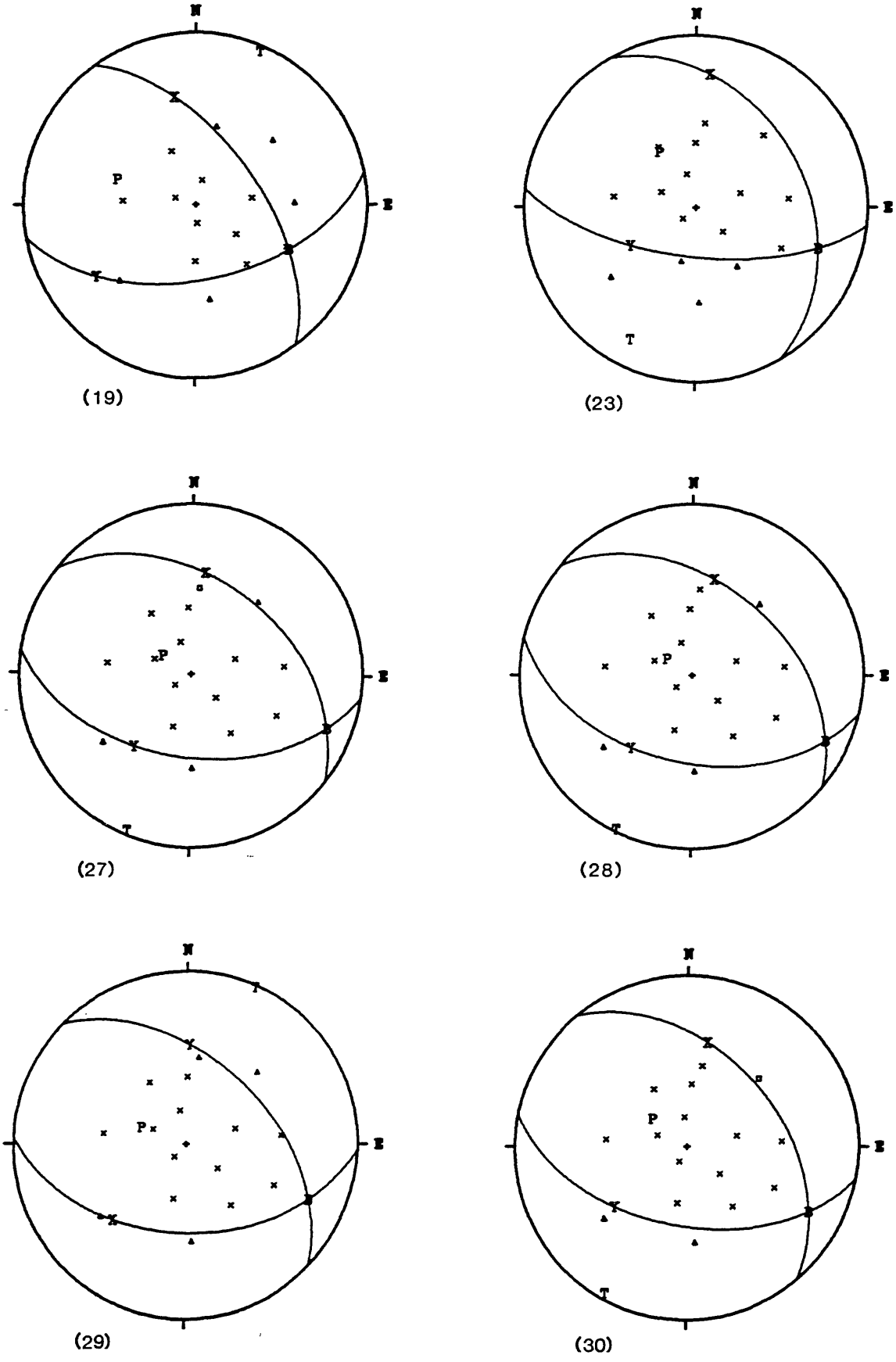

Figure 7. (b) Type 3 aftershock focal mechanism solutions.

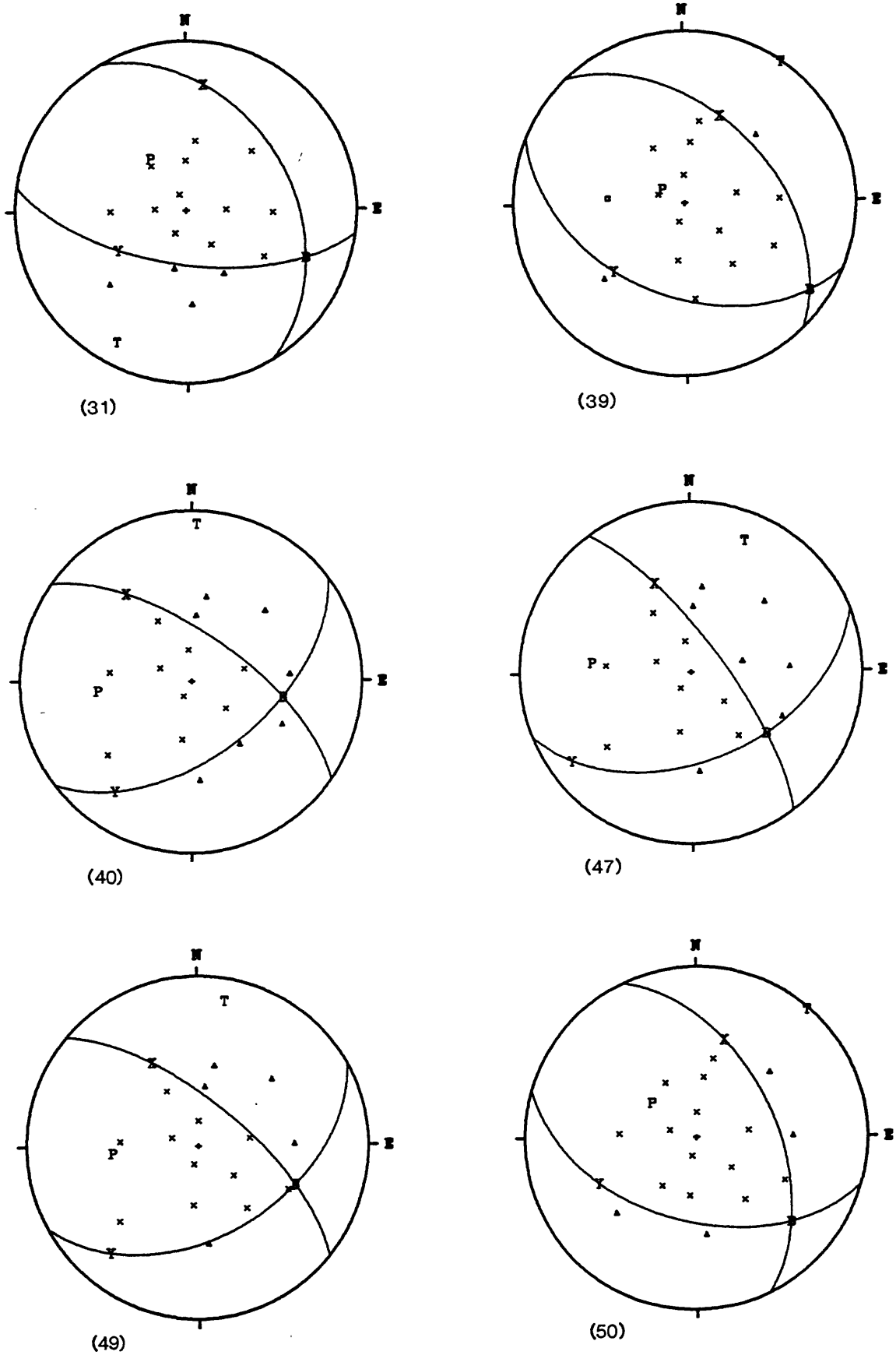

Figure 7. (b) Type 3 aftershock focal mechanism solutions (continued).

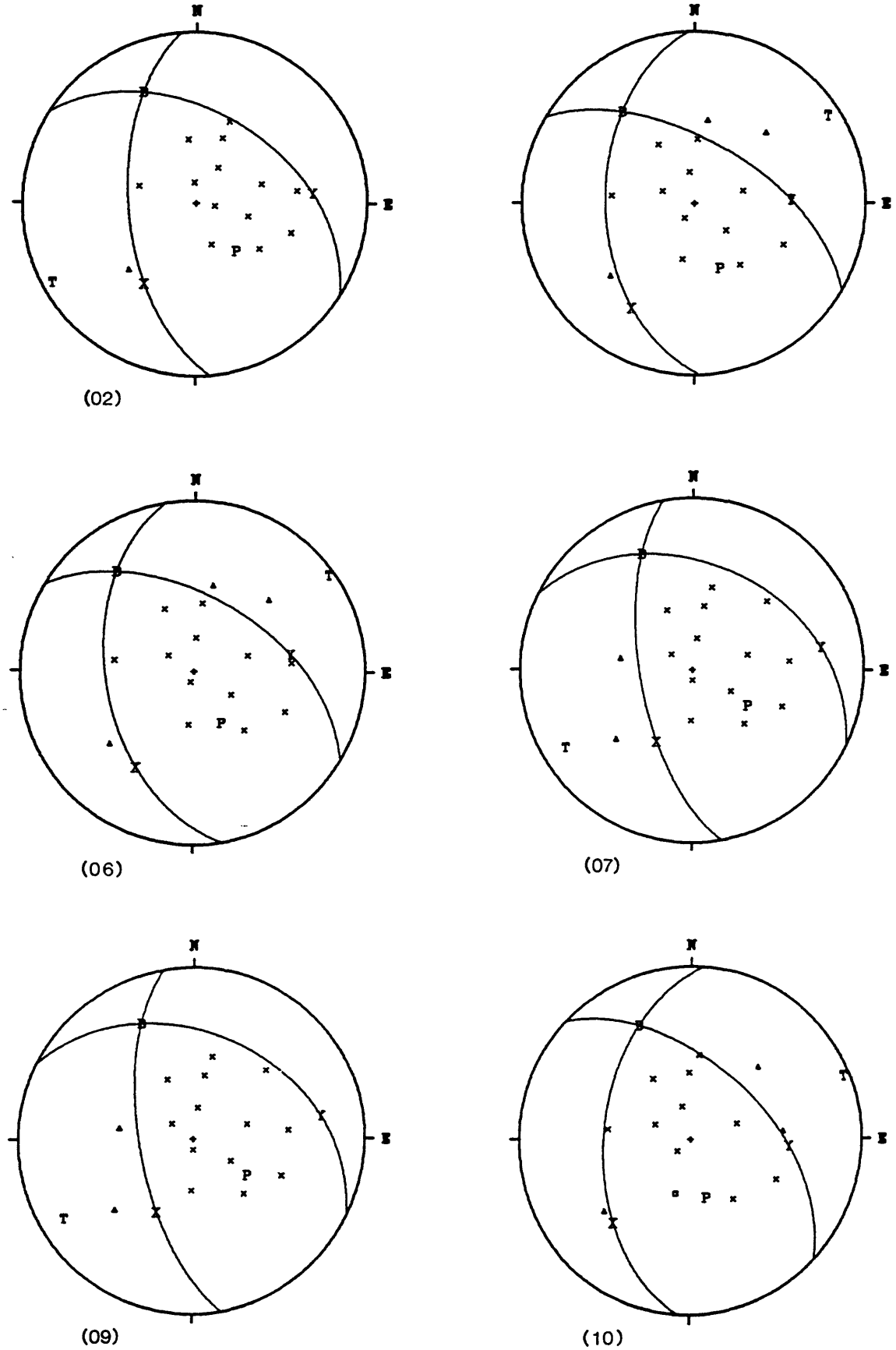

Figure 7. (b) Type 4 aftershock focal mechanism solutions.

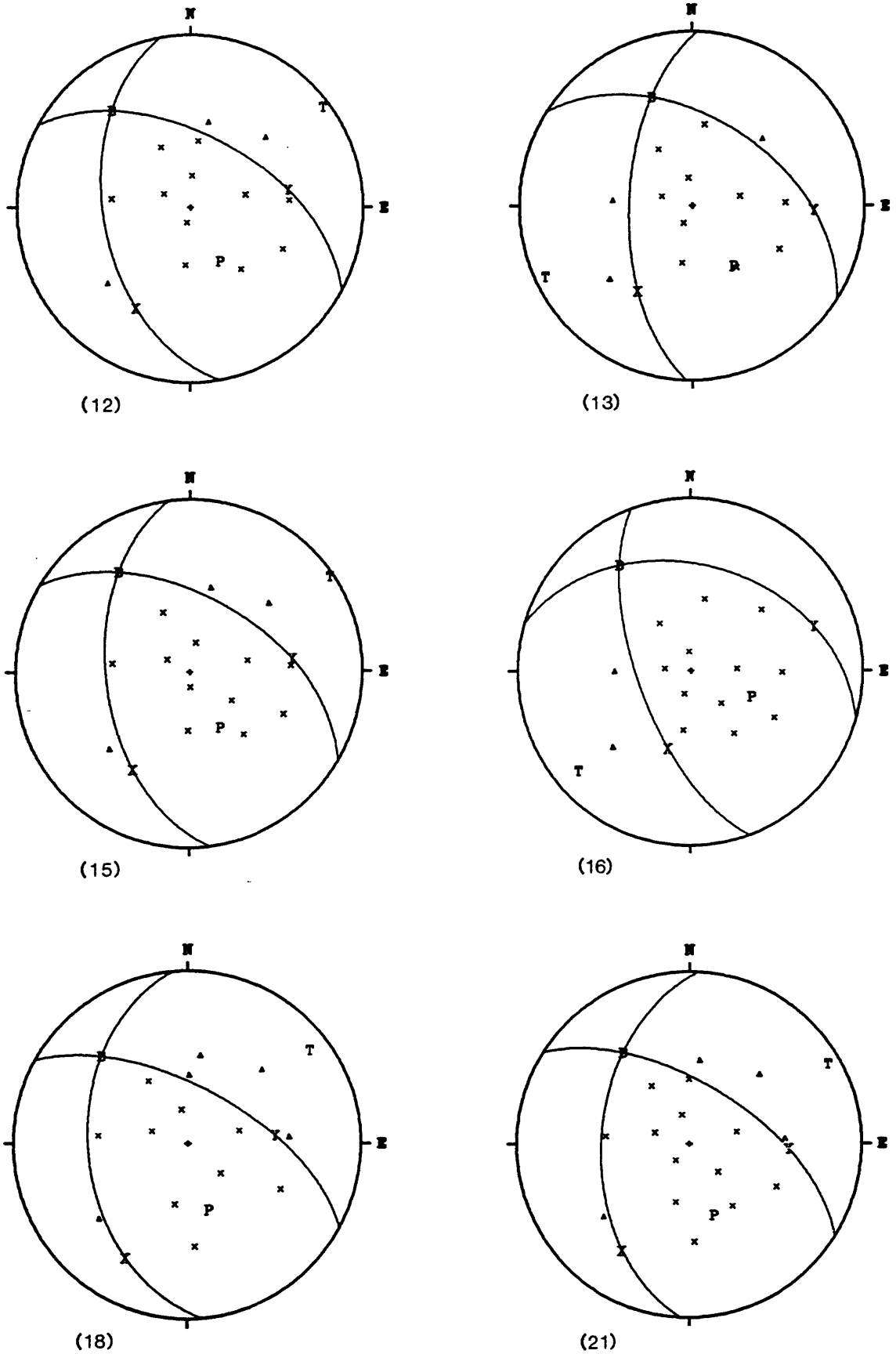

Figure 7. (b) Type 4 aftershock focal mechanism solutions (continued).

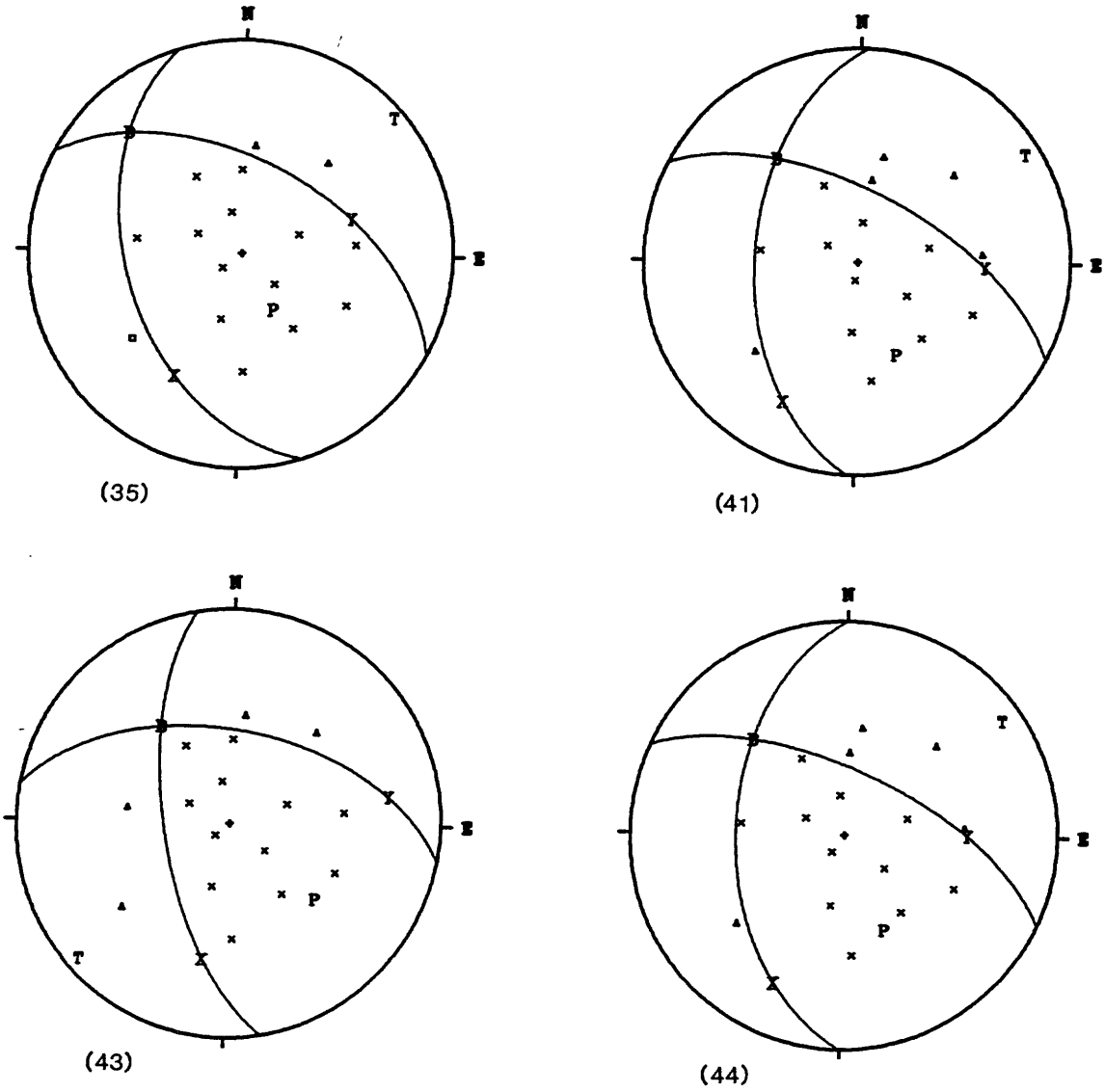

Figure 7. (b) Type 4 aftershock focal mechanism solutions (continued). Types 1, 2, 3, and 4 solutions are lower hemisphere, equal area projections. Two digit number enclosed by parentheses below sphere is aftershock designator keyed to tables 3 and 5. *P* and *T* indicate approximate location of *P*- and *T*-axes.

TABLE 6a.–Summary of aftershock focal mechanism characteristics

Type	Dominant Mode of Faulting	P-Axes Orientations	T-Axes Orientations
1	Strike-Slip	WNW-subhorizontal	NNE-subhorizontal
2	Strike-slip	NW-intermediate	NE-subhorizontal
3	Normal	WNW-intermediate to subvertical	NNE-subhorizontal
4	Normal	NW-intermediate	NE-subhorizontal

TABLE 6b.–Summary of maximum and minimum compressive stress (P- and T-axes) distribution for different type mechanisms

	P-axes		T-axes			
Focal Mech Soln Type	Range of Azimuth (deg)	Range of Plunge (deg)	Range of Azimuth (deg)	Range of Plunge (deg)	Avg azimuth (deg)	No. of Events
Main Shock	N 71 W	24.7	N 23 E	08.5	N 23 E	1
1	N 67 W - N 52 W S 75 E - N 68 E	03 - 26 03 - 30	N 13 E - N 38 E S 17 W - S 27 W	00 - 25 01 - 03	N 23 E S 23 W	12
2	— S 46 E - S 80 E	— 29 - 37	N 42 E - N 57 E S 26 W	07 - 20 24	N 52 E S 52 W	7
3	S 87 W - N 33 W —	42 - 78 —	N 92 E - N 41 E S 22 W - S 29 W	01 - 18 02 - 18	N 24 E S 24 W	12
4	— S 14 E - S 68 E	— 45 - 65	N 48 E - N 68 E N 47 W - S 65 W	04 - 13 08 - 15	N 56 E S 56 W	16

mechanisms are normal faulting type 3 and during that time (32 hours) there are no type 4. The final 17 mechanisms are rather evenly distributed in type across the remaining 79-hour time span. It is important to recall here that our aftershock locations really began about four days after the mainshock when the optimum distribution of seismographs was in place. By that time, a large number of normal faulting aftershocks were occurring following the mostly strike-slip mainshock.

TECTONIC SETTING

The core of the Laramie Mountain Range primarily consists of Precambrian anorthosites and granite (Middle Proterozoic) to the south and granitic rocks of the Archean Laramie batholith to the north, uplifted during the late Cretaceous - early Tertiary deformation of the Laramide orogeny. Bounded on the east by the Denver Basin and on the west by the Laramie Basin, the uplift forms a nearly linear north-south feature somewhat arcuate to the west at the northern terminus (see fig. 8). Located in southeastern Wyoming, the mountains are part of the Rocky Mountain Front which is the morphological boundary between the gently sloping Great Plains to the east and basement uplifts of the Rocky Mountains. Laramide structures have been discussed in great detail by many investigators. Some of the more recent studies include those by Allmendinger and others (1982), Brewer and others (1982), King and Brewer (1983), and Gries (1983); a compilation of the mapped regional geology has been published by Love and Christiansen (1985).

Uplifts of the Rocky Mountain foreland ("Laramide") formed interior from an active eastward subducting plate margin at distances of 1,000 - 1,500 km. Work by Coney (1976) and Dickerson and Snyder (1978) on the relationships of volcano patterns to plate tectonics suggests that Laramide basement deformation in Wyoming and Colorado may have occurred above a nearly horizontal subducting plate. Unanswered questions still remain about how the basement uplifts evolved in Wyoming, whether or not they developed along moderately low-angle thrusts (Brewer and others, 1982; King and Brewer, 1983) or as a result of more complex models with steeper-dipping faults and various directions of crustal shortening (Hamilton, 1981; Chapin and Cather, 1981; and Gries, 1983).

Several faults with known or suspected Miocene to Recent displacements have been identified for Wyoming and plotted on the State map (scale 1:500,000) by Witkind (1975). None of these faults are in nor are they closely adjacent to the northern Laramie Mountains.

LOCAL GEOLOGY

A geologic field investigation was conducted following the 18 October 84 main shock to provide some potentially useful surface constraints that may be related to fault movement during the study earthquake or its prehistoric ancestors. The observations are from three areas in the epicentral region and, in order of importance, are referred to as areas 1, 2, and 3 on figure 9.

Geologic lineaments. Three surficial lineaments near the earthquake source include: (a) the north-south striking Fortymile Flat-Downy Park Tertiary-gravel-filled valleys traversed by the Old Fort Fetterman road. It cuts entirely across the mountain range (through 1, figure 9; e.g. see U.S. Geological Survey, 1981) and will be referred to as the Old Fort Fetterman road lineament; (b) a north 65° - 75° east-striking feature that passes through La Bonte canyon (no.2, figure 9) we refer to as the La Bonte canyon lineament, extends west-southwest and may align with some basin faults mapped to the west by Harshman (1968). In La Bonte Canyon, this lineament shows an apparent 1 km right lateral offset of two perpendicular tributaries (Big Bear Canyon and Curtis Gulch, e.g. see U.S. Geological Survey, 1981). Other nearby mountain lineaments to the north and south are subparallel to La Bonte Canyon; and (c) an east-west striking alignment along lower Manse Creek through 3, figure 9, will be referred to as the Manse Creek lineament.

Surface Investigations. Geologic studies of the above three lineaments developed the following ground truths (and ground "maybes") for each. All work was performed by G. Snyder in 1985 subsequent to an aerial reconnaissance by Snyder and R. Bucknam less than 24 hours following the main shock.

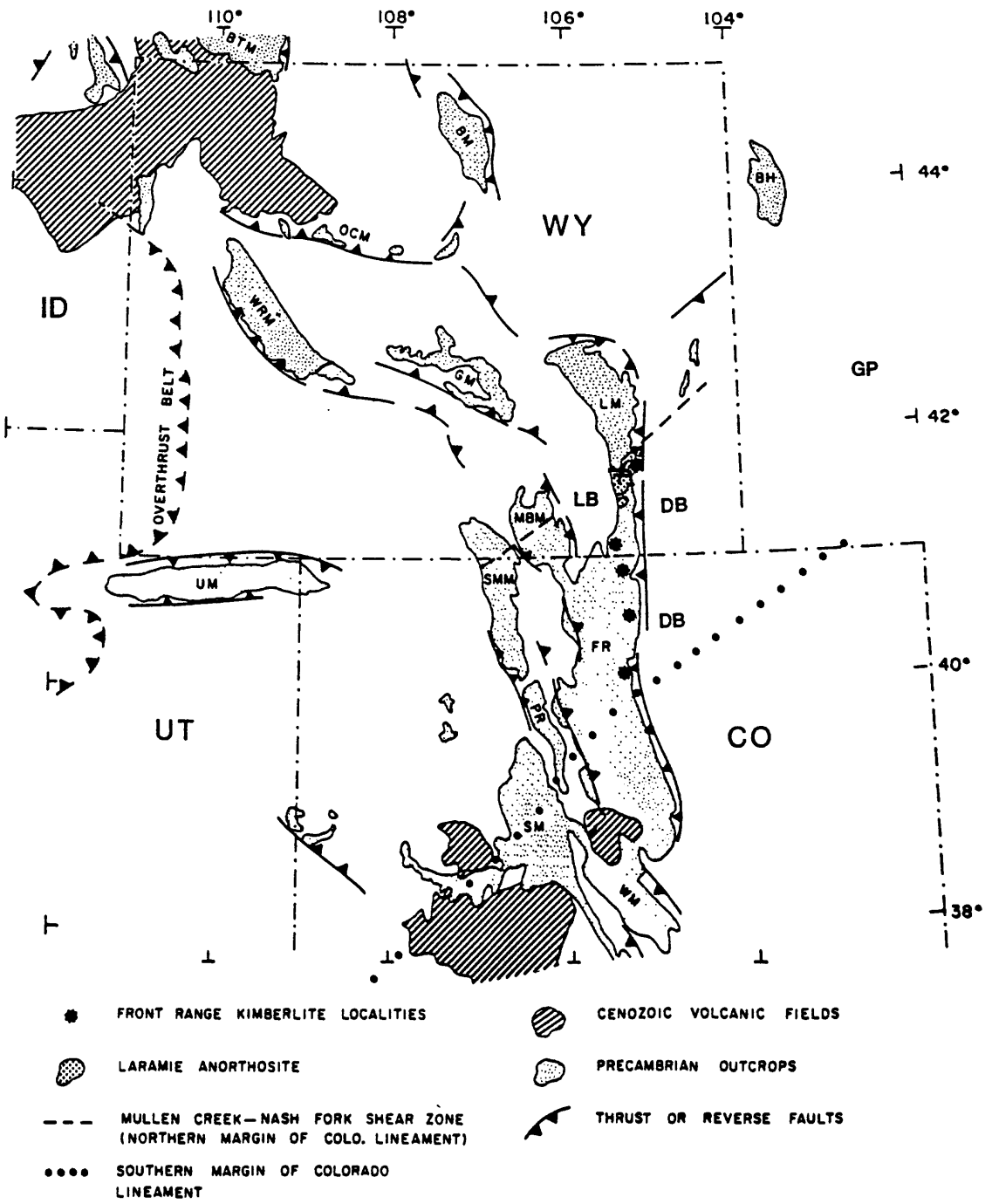

Figure 8. Major geological features in the vicinity of 18 October 1984 Laramie Mountains earthquake. Map is modified from Brewer and others, 1982. Physiographic features are: BH, Black Hills; BM, Bighorn Mountains; BTM, Beartooth Mountains; DB, Denver Basin; FR, Front Range; GM, Granite Mountains; GP, Great Plains; LB, Laramie Basin; LM, Laramie Mountains; MBM, Medicine Bow Mountains; OCM, Owl Creek Mountains; PR, Park Range; SM, Sawatch Mountains; SMM, Sierra Madre Mountains; WM, Wet Mountains; WRM, Wind River Mountains; VM, Vista Mountains.

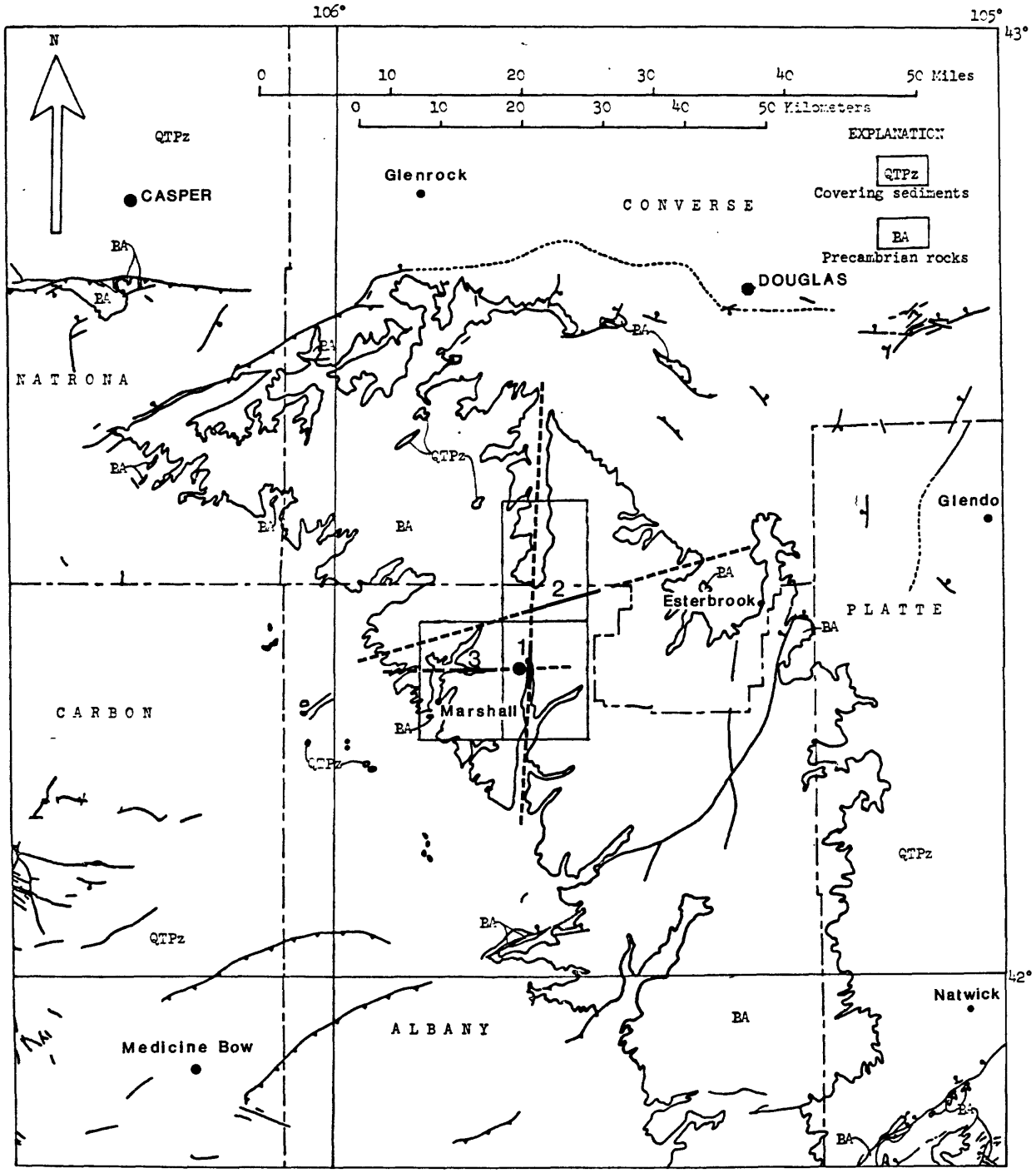

Figure 9. Geologic map and location of lineaments in the vicinity of 1984 earthquake. 1. "Gravel pit" location on Old Fort Fetterman road lineament with exposures of granite and Tertiary north-striking fault planes, Toltec quadrangle (see photographs in figures 10 (a), (b), and (c)); 2. La Bonte Canyon lineament, School Section quadrangle, which had not had localized fault movement subsequent to intrusion of four Precambrian diabase dikes crossing lineament; 3. Manse Creek lineament, Marshall quadrangle, where 50 m diabase dike may have 0.25 km left lateral offset on possible east-west buried Tertiary fault (?). Solid dot near intersection of Old Fort Fetterman road and Manse Creek lineaments is location of aftershock sequence and probably the main shock. Geology from Love and Christiansen (1985).

a. Old Fort Fetterman road lineament. A "gravel pit", labeled on the Toltec 7½-minute quadrangle sheet west of Old Fort Fetterman road (NW¼ sec. 10, T. 27 N., R. 74 W.), is really an exposure of crumbly to shattered to closely jointed granite of the Archean Laramie batholith described by Condie (1969). Here, it is a friable rock easily removed by bulldozer or backhoe without blasting. Nearly vertical north and northwest walls of the pit exposed two zones of fault gouge, as shown by photographs in figures 10a, b, and c.

Another (unlabeled) "gravel pit" was once worked in similarly crumbly granite about 1.5 km due north of the pit shown on the map. This second pit is now slumped or 'dozed over but granite breccia fragments and slumped quartz and magnetite veins were visible at the surface in 1985. The second pit reinforces evidence found in the first, suggesting that the west side of the Old Fort Fetterman road lineament is structurally controlled by a steep north-south striking Tertiary (?) fault. To the south 17.5 km on the Cottonwood 7½-minute quadrangle (SW¼ sec. 34, T. 26 N., R. 74 W.), Pennsylvanian age Casper (?) sandstone was observed in probable sedimentary contact with granite on the east side of the valley suggesting that the resultant movement on an Old Fort Fetterman road fault was east side down.

b. La Bonte Canyon lineament. In an area mainly in the southern part of School Section Mountain 7½-minute quadrangle, granite of the Laramie batholith is cut by sparse 20-m-wide N. 30° - 50° E.-striking, near-vertical diabase dikes that are traceable for several kilometers. In the 8-km stretch between Old Fort Fetterman road and the Curtis Gulch campground, four such diabase dikes were mapped continuously both north and south of La Bonte Canyon, one for 3.5 km. The dikes are not directly dated but similar dikes elsewhere in the Laramie Mountains are recognized as late Archean or early Proterozoic. Bedrock beneath the 20 - 70 m-wide canyon alluvium could not be observed but it is very unlikely that the alluvium hides any younger Phanerozoic fault gouge because the older, cross-cutting dikes have clearly <u>not</u> been offset. From the above evidence we must conclude that the La Bonte Canyon lineament is most likely controlled by a closely spaced post-diabase dike set and is not a fault zone.

c. Manse Creek lineament. The area examined was near the Manse Creek ranch, Marshall 7½-minute quadrangle (sec. 2, T. 27 N., R. 75 W.). A high N. 30° E. trending ridge beginning about 0.5 km west of the ranch is underlain by a distinctive near-vertical course clinopyroxene diabase dike cutting granite of the Laramie batholith. The dike ridge appears to be continuous for at least 4.5 km in a N. 30° E. direction northeast of Manse Creek. Near the southwest end of the ridge there is a place where both contacts of the dike are closely controlled (within one or two m) and the paced width of the dike at that point is 50 m.

The Manse Creek alluvium and higher terrace gravels (Tertiary?) obscure the Precambrian rocks across an east-trending valley about 0.5 km in width. South of the alluvium a near-vertical course clinopyroxene diabase dike continues in a southwest direction for at least 2 km. Near the northeast end of the dike, a closely controlled width of 49 m was paced. It is most likely that this dike is the same as the one described above on the north side of the valley. If the mapped dike segments closest to Manse Creek are projected out to an east-west line down the center of the Manse Creek lineament, the southwest segment intersects the line about 0.25 km east of where the northeast segment projects. This gives permissible evidence of *left* lateral offset along a hypothetical east-west completely buried (Tertiary?) fault. An alternative interpretation is that the dike curves or has *en echelon* configuration beneath the alluvium of the 0.5-km-wide valley and connects on the bedrock surface or at depth without offset.

<u>Summary of field geologic results.</u> A field investigation of three geologic lineaments in the epicentral region produced no evidence indicating Quaternary fault displacements. Two of the lineaments (Old Fort Fetterman road and Le Bonte canyon) are well-developed, deeply entrenched features that may have resulted form jointing within the granitic rocks of the Laramie batholith. Fault gouge discovered in two gravel pits west of Old Fort Fetterman road suggests that the structure on the west side of the Old Fort Fetterman road lineament is at least partly controlled by a steeply dipping north-south striking Tertiary (?) fault, east side down.

Figure 10. (a) Geologic hammer beside a 10-inch-wide N. 25° E., 80° NW fault gouge-breccia zone, north wall of "gravel pit" west of Old Fort Fetterman road, location shown in figure 9 (photograph taken by G.L. Snyder).

Figure 10. (b) Open Brunton compass beside 4-inch-wide iron-stained N.-S., 70° W. fault gouge zone on northwest wall of same pit, figure 10(a) (photograph taken by G.L. Snyder).

Figure 10. (c) Overall view of north and northwest walls of "gravel pit" (fig. 9), hammer and Brunton in same position as in (a) and (b) (photograph taken by G.L. Snyder).

DISCUSSION

Several aspects of the Laramie Mountains shock are of particular interest, two of the most noteworthy being a focal depth of more than 20 km and a larger than usual felt area for an m_b 5.4 Western United States earthquake. An examination of catalogs of instrumentally located earthquake hypocenters forseismicity within the conterminous United States (specifically, the Earthquake Data Base System, U.S. Geological Survey National Earthquake Information Center, Golden, Colorado) suggests that intraplate earthquakes of magnitude ≥ 5.0 usually occur at depths between 5 and 15 km. One exception prior to 1984 was a magnitude m_bL_g = 5.5 event in southern Illinois on 9 November 1968 located at a depth of about 22 km (Herrman, 1979; Gordon, 1988). Also, since 1968, foci between 20 and 24 km have been computed for smaller magnitude earthquakes (m_bL_g 3.0 - 3.5) originating in that same geographic area (Gordon, 1988). Wong and Chapman (1990) have recently compiled an account of small earthquakes ($M_L \leq 4.6$) in the western United States (northwestern New Mexico, Paradox Basin of Utah and Colorado, northeastern Utah, and several areas in California) that have occurred below 20 km. Other reports of microseismicity (magnitudes < 3.0) occurring as deep as 30 km or more, have been published for areas where good local/regional network coverage exists such as in Utah (Richins and others, 1984; Brown and others, 1986), southeastern Nevada (Rogers and others, 1987; Harmsen and Rogers, 1987), and the southeastern United States (Sibol and others, 1987). Thus, intraplate focal depths greater than 20 km are somewhat unusual but certainly not rare for microseismicity and earthquakes as large as M_L 4.6. However, the Laramie Mountains earthquake is the deepest known intraplate event west of the Mississippi River with a magnitude greater than 5.0.

The Laramie Mountains focal depth of 22 km, estimated by Harvard University is in close agreement with the clustering of aftershock foci between 21 and 24 km. On the basis of the depth range of aftershocks alone, one could assume that the main shock must have occurred below 21 km. A recently published report on crustal velocities in Wyoming and the southern Rocky Mountains (Prodehl and Lipman, 1989) suggests a three-layer model (4.0 km/sec, 0-2 km; 6.3 km/sec, 2-30 km; 6.9 km/sec, 30-38 km) over a 7.9 km/sec half-space *with a* V_p/V_s ratio of 1.67, may be representative of the actual regional/local velocity structure. Our testing of this model indicated that slightly deeper aftershock foci (about 0.3 km overall) result while the HYPOELLIPSE epicenters and location error statistics remain virtually unchanged. This test assured us that our single-layer over a half-space model and slightly higher V_p/V_s ratio introduced no significant errors in the relative aftershock hypocenters. Thus, for both models, all aftershocks were located at depths greater than 20 km.

It is well known that the anelastic attenuation of seismic energy in the crust and upper mantle of the continental United States is greater in the west than it is in the central and eastern regions. As a result, intermediate magnitude earthquakes in the west do not cause the large felt areas commonly associated with equivalent magnitude shocks in the mid-continent and in the east. For example, comparison curves of the log felt area versus magnitude for m_b 4.0 - 5.5 earthquakes in California (CA) and in the central region (CR) demonstrate a significant difference. Also indicated is an increase in the ratio of felt areas (CR felt area/CA felt area) from about 11 to 28 over a corresponding magnitude increase from m_b = 5.0 to m_b = 5.5 (see Nuttli and Zollweg, 1974). The felt area (287,000 km^2) measured by Stover (1985) for the Laramie Mountains event appears to be somewhere between what would be expected in the CR and in CA, the felt area being roughly 3.4 times greater than expected for CA and about 6.2 times less than expected for the CR. This large felt area may also be an artifact of the "anomalously" deep focal depth. In Europe for example, macroseismic observations suggest that for a given epicentral intensity, deeper earthquakes are likely to be felt more widely than those with a shallow depth of focus (e.g., see Blake, 1941; Sponheuer, 1960).

Our efforts to spatially associate different types of aftershock focal mechanisms with local geologic and/or physiographic features were not successful. None of the observed lineaments or faults (?) could be positively associated, within the resolution of our data, to the hypocentral source. Given the depth of this shock, the lack of surface deformation is not unexpected. Rather, what we primarily sought was evidence of surficial movements due to prehistoric earthquakes that were ancestral to the study event.

Nevertheless, valuable information about the state of stress in the epicentral region was obtained from the 47 single-event aftershock mechanisms. Two classes of mechanisms were identified (normal and

strike-slip) which were ultimately subdivided into four types. Inasmuch as only 16 polarities, maximum, were used to determine any one particular focal mechanism solution, there may be a considerable amount of freedom in placement of at least one nodal plane for some events. However, it appears clear from these mechanisms that two directions of extensional stress were active, north-northeast and northeast (see table 6a and fig. 7a), during the period of aftershock monitoring. Approximately 30° separates the average azimuthal direction of the *T*-axes for the main shock and 24 type 1 and 3 aftershocks compared to the average azimuth for the *T*-axes of the remaining 23 type 2 and 4 aftershocks. These variations in the stress field and the close proximity of most aftershocks suggest that displacement on two separate fault systems or segments may have been involved in the main shock episode. Alternatively, the main shock may have perturbed the local stress field resulting in conjugate fault motions adjacent to the causal fault but at a somewhat different strike and/or dip.

On a regional scale, the azimuthal direction of the *T*-axes determined by focal mechanisms for the main shock and aftershocks is reasonably consistent with the northeasterly horizontal minimum compressive stress orientation inferred by Zoback and Zoback (1980, 1989) for the southern Rocky Mountains. Borehole breakout data in the Denver Basin south of 41° latitude (Dart, 1985), have shown that the extensional stress field there may be more easterly directed (~N. 60° E. - N. 80° E.). Data to the north and west also indicate general agreement with the Laramie Mountains but, like the Denver Basin, display a more clockwise rotation (~20° - 30°) of the minimum compressive stress. Eastward, no reliable stress orientations are available for over 800 km (Zoback and Zoback, 1989).

Finally, a comparison of Wyoming's 90 year average rate of one $MMI_0 \geq V$ earthquake (outside Yellowstone Park) every 3.2 years against the accelerated 1984 value of four/year provides a good example of the range of variation that can occur within such average rates. Seismic hazard analysis uses these average rates for routine hazard evaluation but the analyst and others in the user community should be aware of the possible extreme variations in those rates, over the short-term, as exemplified here.

SUMMARY

To summarize, our aftershock investigation of the Laramie Mountains earthquake has provided the following results:

(1) The majority of the 47 locally recorded aftershocks occupy a small cylindrical volume roughly 4 km in diameter by 5 km in height;

(2) Most of the aftershocks occurred between about 21 and 24 km in depth;

(3) Based on the aftershock depths, the main shock probably occurred below 21 km and is therefore one of the deepest known earthquakes of m_b = 5.4 (M_L = 5.5) within the continental interior; also, the associated intensity-felt area (287,000 km^2) was larger than expected for that magnitude;

(4) Two directions of horizontal extensional stress (about N. 20° E. and N. 50°E.) are associated with the aftershock sequence and in general agreement with the regional northeasterly stress distribution.

ACKNOWLEDGEMENTS

The authors are grateful to Tom Bice, Kathy Haller, Dave Hampson, and Regina Henrisey for their assistance in the field. Margaret Hopper and Susan Rhea critically reviewed the manuscript and made helpful comments and suggestions. The project was partially funded by the Bureau of Reclamation, Engineering and Research Center.

REFERENCES

Aki, K., 1966, Generation and propagation of G-waves from the Miigata earthquake of June 16, 1964, Part 2. Estimation of earthquake moment, released energy, and stress-strain drop from the G-wave spectrum: *Bulletin of the Earthquake Research Institute, University of Tokyo*, **44**, p. 73-88.

Allmendinger, R.W., Brewer, J.A., Brown, L.D., Kaufman, S., Oliver, J.E., and Houston, R.S., 1982, COCORP profiling across the Rocky Mountain Front in southern Wyoming, Part 2--Precambrian basement structure and its influence on Laramide deformation: *Geol. Soc. Am.* **93**, p. 1253-1263.

Blake, A., 1941, On the estimation of focal depth from macroseismic data, *Bull. Seism. Soc. Am.*, **31**, 225-232.

Brewer, J.A., Allmendiner, R.W., Brown, L.D., Oliver, J.E., and Kaufman, S., 1982, COCORP profiling across the Rocky Mountain Front in southern Wyoming, Part 1--Larmide structure: *Geol. Soc. Am.* **93**, p. 1242-1252.

Brown, E.D., Arabasz, W.J., Pechmann, J.C., McPherson, E., Hall, L.L., Oehmich, P.J., and Hathaway, G.M., 1986, Earthquake data for the Utah region, January 1, 1981 to December 31, 1983, *University of Utah Seismograph Stations, Department of Geology and Geophysics, University of Utah, Salt Lake City, Utah*, 84112-1183, 111 pp.

Brune, J.N., 1970, Tectonic stress and the spectra of seismic shear waves from earthquakes: *J. Geophys. Res.*, **75**, p. 4997-5009.

Chapin, C.E., and Cather, S.M., 1981, Eocene tectonics and sedimentation in the Colorado Plateau--Rocky Mountain area, *in* Dickinson, W.R., and Payne, W.D., (eds.), Relations of Tectonics to Ore Deposits in the southern Cordillera: *Arizona Geological Society Digest*, **14**, p. 173-198.

Coffman, J.L., von Hake, C.A., and Stover, C.W., (ed's), 1982, Earthquake History of the United States, Publication 41-1, Revised Edition (through 1970) with Supplement (1971 - 80): *U.S. Department of Commerce, National Oceanic and Atmospheric Administration* and *U.S. Department of the Interior, Geological Survey*, Boulder, CO, 258 pp.

Condie, K.E., 1969, Petrology and geochemistry of the Laramie batholith and related metamorphic rocks of Precambrian age, eastern Wyoming: *Geol. Soc. Am.* **80**, p. 57-82.

Coney, P.J., 1976, Plate tectonics and the Laramide orogeny: *New Mexico Geological Society Special Publication* 6, p. 5-10.

Dart, R., 1985, Horizontal stress directions in the Denver and Illinois Basins from the orientations of borehole breakouts: *U.S. Geol. Surv. Open-File Report* **85-722**, 41 p.

Dickinson, W.R., and Snyder, W.S., 1978, Plate tectonics of the Laramide orogeny, *in* Matthews, v., III, (ed.), Laramide Folding Associated with Basement Block Faulting in the Western United States: *Geol. Soc. Am. Mem.* **151**, 355-366.

Dziewonski, A.M., Chou, T.A., and Woodhouse, J.H., 1981, Determination of earthquake source parameters from waveform data for studies of global and regional seismicity: *J. Geophys. Res.* **68**, 2823-2852.

Gordon, D.W., 1987, Seismicity and tectonics in the Wyoming foreland [abs.]: SRL, **58, no. 4**, p. 97-98.

Gordon, D.W., 1988, Revised instrumental hypocenters and correlation of earthquake locations and tectonics in the Central United States: *U.S. Geol. Surv. Prof. Paper* **1364**, 69 pp.

Gries, R., 1983, North-south compression of Rocky Mountain foreland structures, *in* Lowell, J.D., (ed.), Rocky Mountain Foreland Basins and Uplifts: *Rocky Mountain Association of Geologists Symposium*, p. 9-32.

Hamilton, W., 1981, Plate-tectonic mechanism of Laramide deformation: *Contr. Geology*, **19**, p. 87-92.

Harmsen, S.C., and Rogers, A.M., 1987, Earthquake location data for the southern Great Basin of Nevada and California: 1984 through 1986, *U.S. Geol. Surv. Open-File Report* **87-596**, 92 pp.

Harshman, E.N., 1968, *U.S. Geol. Surv. I-Map* **539**

Herrmann, R.B., Park, S-K, and Wang, C-J, 1981, The Denver earthquakes of 1967-1968: *Bull. Seism. Soc. Am.* **71**, no. 3, 731-745.

Herrmann, R.B., 1979, Surface wave focal mechanisms for eastern North America earthquakes with tectonic implications: *J. Geophys. Res.*, **84**, p. 3543-3552.

Jackson, W.H., and Pakiser, L.C., 1965, Seismic study of crustal structure in the southern Rocky Mountains: *U.S. Geol. Surv. Prof. Paper* **525-D**, p. D-85-D92.

King, G., and Brewer, J., 1983, Fault related folding near the Wind River thrust, Wyoming, USA: *Nature*, **306**, p. 147-150.

Lahr, J.C., 1984, HYPOELLIPSE/VAX--A computer program for determining local earthquake hypocenter parameters, magnitude, and first motion pattern: *U.S. Geol. Surv. Open-File Report* **84-519**, 60 p.

Langer, C.J., Martin, R.A., and Wood, C.K., 1985, Preliminary results of the aftershock investigation of the October 18, 1984, Laramie Mountains, Wyoming, earthquake [abs.]: *Earthquake Notes*, **55**, p. 24.

Lee, W.H.K. and Stewart, S.W., 1981, Principles and Applications of Microearthquake Networks, *Academic Press*, New York, NY, 293 pp.

Love, J.D. and Christiansen, A.C., 1985, Geologic map of Wyoming, scale 1:500,000, 3 sheets, sold by *Branch of Distribution, U.S. Geological Survey*, Box 25286, Denver Federal Center, Denver, CO 80225.

Mokler, A.J., 1923, History of Natrona County, Wyoming 1888-1922, R.R. Donnelley & Sons Company, The Lakeside Press, Chicago, IL., p. 72-74.

Nuttli, O., and Zollweg, J.E., 1974, The relation between felt area and magnitude for central United States earthquakes, *Bull. Seism Soc. Am.*, **64**, 73-85.

Prodehl, C. and Lipman, P.W., 1989, Crustal structure of the Rocky Maountain region, *in* Pakiser, L.C. and Mooney, W.D., Geophysical Framework of the Continental United States: Geological Soc. of America Memoir 172, p. 249-284.

Prodehl, C., and Pakiser, L.C., 1980, Crustal structure of the southern Rocky Mountain from seismic measurements: *Geol. Soc. Am.* **91**, p. 147-155.

Reagor, B.G., Stover, C.W., and Algermissen, S.T., 1985, Seismicity map of the state of Wyoming: *U.S. Geol. Surv. Miscellaneous Field Studies Map* **MF-178**, 1:100,000 scale, 1 sheet.

Reagor, G., and Stover, C.W., 1990, Earthquake Data Base System (EDBS): *U.S. Department of Interior, Geological Survey* (unpublished).

Richins, W.D., Arabasz, W.J., Hathaway, G.M., Ochmich, P.J., and Sells, L.L., 1984, Earthquake data for the Utah region, January 1, 1981 to December 31, 1983, *University of Utah Seismograph Stations, Department of Geology and Geophysics, University of Utah, Salt Lake City, Utah*, 84112-1183, 111 pp.

Rogers, A.M., Harmsen, S.C., and Meremonte, M.E., 1987, Evaluation of the seismicity of the southern Great Basin and its relationship to the tectonic framework of the region, *U.S. Geol. Surv. Open-File Report* **87-408**, 196 pp.

Sibol, M.S., Bollinger, G.A., and Mathena, E.C., 1987, Seismicity of the southeastern United States: *Southeastern U.S. Network Bulletin* **No. 20**, published by the Seismological Observatory, Virginia Polytechnic Institute and State University, Blacksburg, VA., 24061.

Smith, R.B., 1978, Seismicity, crustal structure, and intraplate tectonics of the Eastern Cordillera *in* Cenozoic Tectonics and Regional Geophysics of the Western Cordillera, R.B. Smith and G.P. Eaton, (Eds.): *Geol. Soc. Am. Mem.* **152**, 111-144.

Sponheuer, W., 1960, Methoden zur Herdtiefenbestimmung in der Madroseismik, *Freibergerforschungshefte*, c 88.

Stover, C.W., 1985, Preliminary Isoseismal and intensity distribution for the Laramie Mountains, Wyoming earthquake of October 18, 1984: *U.S. Geol. Surv. Open-File Report* **85-137**, 9 pp.

Stover, C.W., 1988, United States Earthquakes, 1984: *U.S. Geol. Surv. Bull.* **1862**, 179 pp.

U.S. Department of Commerce, compiled by R.R. Bodle, 1946, United States Earthquakes, 1944, Serial No. 682: issued by the Coast and Geodetic Survey through United States Government Printing Office, Washington 25, D.C.

U.S. Department of Commerce, compiled by L.M. Murphy and W.K. Cloud, 1956, United States Earthquakes, 1954, Serial No. 793: issued by the Coast and Geodetic Survey through United States Government Printing Office, Washington 25, D.C., 115 pp.

U.S. Department of Commerce, compiled by R.A. Eppley and W.K. Cloud, 1961, United States Earthquakes, 1959, issued by the Coast and Geodetic Survey, through the United States Government Printing Office, Washington 25, D.C., 115 pp.

U.S. Department of Commerce, compiled by C.A. von Hake and W.K. Cloud, 1965, United States Earthquakes, 1963, issued by the Coast and Geodetic Survey through United States Government Printing Office, Washington, D.C. 20402, 69 pp.

U.S. Department of Commerce, Environmental Science Services Administration, compiled by C.A. von Hake and W.K. Cloud, 1966, United States Earthquakes, 1964, issued by the Coast and Geodetic Survey through United States Government Printing Office, Washington D.C. 20402, 91 pp.

U.S. Department of Commerce, Environmental Science Services Administration, 1968, United States Earthquakes, 1928-1935: reissued by the Coast and Geodetic Survey, National Earthquake Information Center, U.S. Government Printing Office, Washington D.C., 20402.

U.S. Department of Commerce, Environmental Science Services Administration, 1969, United States Earthquakes, 1936-1940: reissued by the Coast and Geodetic Survey, National Earthquake Information Center, U.S. Government Printing Office, Washington D.C., 20402.

U.S. Department of Commerce and U.S. Department of Interior, 1975, United States Earthquakes, 1973: Published jointly by the National Oceanic and Atmospheric Administration and U.S. Geological Survey, Boulder, CO, 112 pp.

U.S. Geological Survey, 1981, Douglas, Wyoming, 1:100,000-scale metric map, 30X60 minute quadrangle: Produced by the United States Geological Survey, Denver, CO 80225, 1 sheet.

U.S. Geological Survey, 1984, *Preliminary Determination of Epicenters, Monthly Listings*, October 1984, 23 p.

Witkind, I.J., 1975, Preliminary map showing known and suspected active faults in Wyoming: *U.S. Geol. Surv. Open-File Report* **75-279**, 36 p., with 1:500,000 scale map (1 sheet).

Wong, I.G. and Chapman, D.S., 1990, Deep intraplate earthquakes in the western United States and their relationship to lithospheric temperatures: Bull. Seism. Soc. Am., **80**, 589-599.

Zoback, M.L., and Zoback, M.D., 1980, State of stress in the conterminous United States: *J. Geophys. Res.*, **85**, p. 6113-6156.

Zoback, M.L., and Zoback, M.D., 1989, Tectonic stress field of the continental United States *in* Pakiser, L.C. and Mooney, W.D., Geophysical Framework of the Continental United States: Geological Soc. of America Memoir 172, p. 523-537.